Accepted Manuscript

Synthesis, antiamoebic and molecular docking studies of furan-thiazolidinone hybrids

Mohammad Fawad Ansari, Shadab Miyan Siddiqui, Kamal Ahmad, Fernando Avecilla, Sudhaker Dharavath, Samudrala Gourinath, Amir Azam

PII: S0223-5234(16)30706-1

DOI: 10.1016/j.ejmech.2016.08.053

Reference: EJMECH 8849

To appear in: *European Journal of Medicinal Chemistry*

Received Date: 2 July 2016

Revised Date: 21 August 2016

Accepted Date: 22 August 2016

Please cite this article as: M.F. Ansari, S.M. Siddiqui, K. Ahmad, F. Avecilla, S. Dharavath, S. Gourinath, A. Azam, Synthesis, antiamoebic and molecular docking studies of furan-thiazolidinone hybrids, *European Journal of Medicinal Chemistry* (2016), doi: 10.1016/j.ejmech.2016.08.053.

Synthesis, Antiamoebic and Molecular Docking Studies of Furan-thiazolidinone Hybrids

Mohammad Fawad Ansari[1], Shadab Miyan Siddiqui[1], Kamal Ahmad[2], Fernando Avecilla[3], Sudhaker Dharavath[4], Samudrala Gourinath[4], Amir Azam[1]*

[1]*Department of Chemistry, Jamia Millia Islamia, Jamia Nagar, 110 025, New Delhi, India*

[2]*Centre for Interdisciplinary Research in Basic Science, Jamia Nagar, 110 025, New Delhi, India*

[3]*Departamento de Química Fundamental, Universidade da Coruña, Campus da Zapateira, 15071 A Coruña, Spain.*

[4]*School of Life Sciences, Jawaharlal Nehru University, New Delhi - 110067*

** Corresponding author. Tel.: +91 11 2698 1717/3253;*

fax: +91 11 2698 0229/1232. E-mail address: amir_sumbul@yahoo.co.in (A. Azam)

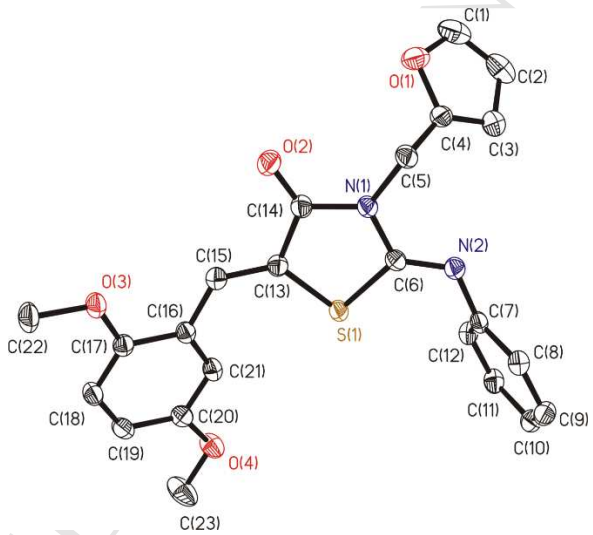

Compound 6

Antiamoebic activity IC_{50} (µM) ± S.D = **0.67±0.042**

Cytotoxicity IC_{50} (µM) ± S.D = **>400** (48 h) **>250** (72h)

Inhibition Assay IC_{50} (µM) = **144.3**

Synthesis, Antiamoebic and Molecular Docking Studies of Furan-thiazolidinone Hybrids

Mohammad Fawad Ansari[1], Shadab Miyan Siddiqui[1], Kamal Ahmad[2], Fernando Avecilla[3], Sudhaker Dharavath[4], Samudrala Gourinath[4], Amir Azam[1]*

[1]*Department of Chemistry, Jamia Millia Islamia, Jamia Nagar, 110 025, New Delhi, India*

[2]*Centre for Interdisciplinary Research in Basic Science, Jamia Nagar, 110 025, New Delhi, India*

[3]*Departamento de Química Fundamental, Universidade da Coruña, Campus da Zapateira, 15071 A Coruña, Spain.*

[4]*School of Life Sciences, Jawaharlal Nehru University, New Delhi - 110067*

Abstract: In continuation of our previous work, a series of furan-thiazolidinone hybrids was prepared by Knoevenagel condensation of 3-(furan-2-ylmethyl)-2-(phenylimino)-1, 3-thiazolidin-4-one with different aryl aldehydes in presence of strong base. Some members of the series exhibited remarkable antiamoebic activity and cell viability. Three compounds **(3**, **6** and **11)** showed excellent binding energy for *Entamoeba histolytica* O-acetyle-L-serine sulfohydrolase and *Entamoeba histolytica* thioredoxin reductase. These compounds demonstrated significant inhibition of O-acetyle-L-serine sulfohydrolase. The promising antiamoebic activity and enzymatic assay of **3**, **6** and **11** make them promising molecules for further lead optimization in the development of novel antiamoebic agents.

Keywords: Furan, Thiazolidinone, Antiamoebic activity, MTT assay, Thioredoxin Reductase.

* *Corresponding author. Tel.: +91 11 2698 1717/3254; fax: +91 11 2698 0229.* E-mail address: amir_sumbul@yahoo.co.in (A. Azam).

1. Introduction

Entamoeba histolytica (*E. histolytica)*, the causative agent of amoebiasis has been listed by the National Institute of Health as a category B priorty biodefense pathogen in the United States [1]. This water borne pathogen possesses contact-dependent cell killing activity and causes up to 100,000 fatalities per annum worldwide [2-3]. There is currently no vaccine against *E. histolytica* [4]. Metronidazole (MNZ) is the first line medicament against amoebiasis but long term use of the drug produces plenty of perilous side effects [5-6]. Furthermore, resistance to MNZ has been reported and the treatment failure may emerge as a major public health issue [7]. *E. histolytica* O-acetyl serine sulfhydrylase (*Eh*OASS) and *E. histolytica* thioredoxin reductase (*Eh*TrR) are two important enzymes that play crucial role in the life cycle of the parasite. The growth and survival of *E. histolytica* depend upon the cysteine biosynthetic pathway [8]. O-acetyl serine sulfhydrylase catalyses the last step of the cysteine biosynthetic pathway. Cysteine, which is the product of this pathway, is the only anti-oxidative thiol in *E. histolytica* and plays significant role in maintaining the redox balance in the organism [9]. *E. histolytica* thioredoxin reductase is also an important enzyme that maintains intracellular redox balance [10]. Thioredoxin reductase (TrR) catalyzes the reversible transfer of reducing equivalents between NADPH and thioredoxin [11-12]. In view of the importance of *E. histolytica* O-acetyl serine sulfhydrylase and *E. histolytica* thioredoxin reductase, these enzymes could be good drug target as both of these enzyme homologues are absent in mammalian hosts.

It has been demonstrated that the additive or even significant synergistic effects can be achieved by molecular hybridization of two or more different medicinally active scaffolds into a single chemical entity [13]. Furan, a well-studied five-membered heterocyclic, has

been accounted to display various biological activities such as antibacterial, antiviral, antifungal, antitumor, antiinflamatory and antiglycemic [14]. Furan constitutes the basic core of antiamoebic drug diloxanide furoate (Figure 1) [15]. In our previous studies, some compounds bearing furan ring in conjugation with other scaffolds have been found to exhibit remarkable antiamoebic activities (Figure 2) [16]. Recently we have synthesized some novel thiazolidinone derivatives starting from 2-methylpropane-1-amine that demonstrated better growth inhibitory potential against *E. histolytica* (Figure 3) [17]. Encouraged by the results of the previous studies [16-17] and the fact that the combination of thiazolidinones with other heterocyclic rings produce various biological activities [18], we hypothesized that the thiazolidinone derivatives incorporating a heterocyclic ring might exhibit synergistic effects. Therefore, in this paper, we herein report the synthesis, antiamoebic activity, molecular docking and enzymatic assay of furan-thiazolidinone hybrids (Figure 4).

2. Results and Discussion

2.1. Chemistry

The synthetic pathway leading to the title compounds (**3-17**) is depicted in Scheme (1). 1-(Furan-2-ylmethyl)-3-phenylthiourea (**1**) was synthesized by reacting phenyl isothiocyanate with furfuryl amine in presence of toluene. Sodium acetate assisted cyclization of compound **1** with chloroacetic acid afforded 3-(furan-2-ylmethyl)-2-(phenylimino)-1, 3-thiazolidin-4-one (**2**). Finally, Knoevenagel condensation of compound **2** with different aryl aldehydes in presence of strong base furnished the target furan-thiazolidinone hybrids (**3-17**). The structures of all the target compounds (**3-17**) were elucidated on the basis of FT-IR, ^{1}H NMR, ^{13}C NMR and ESI-MS. Additional supports for the proposed structure confirmed by X-ray crystallographic studies. The purity of the compounds was confirmed by the elemental analyses.

2.2. Single crystal structure

Single crystal structures of 2, 6, 8, 13 and 15

The asymmetric units of **2, 6, 13** and **15** contain one molecule of furan-thiazolidinone hybrids. The asymmetric unit of 8 contains two molecules of furan-thiazolidinone hybrids and one molecule of cyclohexane. The cyclohexane ring is in a chair form. The furan and phenylimino rings are rotated respect to the carbon atom, C5, and nitrogen atom, N2, respectively, in different forms in the five compounds (Figures 5 to 9). Crystal data and details of the data collection and refinement for the compounds **2, 6, 8, 13** and **15** are mentioned in Table 1. Bond lengths and angles are summarized in supplementary data (Table SI1). In **8**, the presence of intermolecular hydrogen bonds between the two molecules of furan-thiazolidinone hybrids determinate the crystal packing (Table SI2 in supplementary data). In the solid state, the compounds **2** and **8** form π-π stacking interactions between thiazolidinone rings, which are in *anti* cofacial configuration respect to thiazolidinone units (Figures 10 and 11) [19]. The distances between centroids are: $d_{c1\text{-}c2}$ = 3.777 Å [c1 (N1J-C6J-S1J-C13J-C14J), c2 (N1B-C6B-S1B-C13B-C14B) and repeated for other centroids] in 2, and $d_{c3\text{-}c4}$ = 3.562 Å [c3 (N4C-C31C-S2G-C29C-C30C), c4 (N4G-C31G-S2G-C29G-C30G)] and repeated for other centroids] in **8**. In **6**, several π-π stacking interactions between dimethoxybenzylidene and thiazolidinone groups of different frameworks determinate the crystal packing, and form antiparallel dimers, [20] (Figure 12): $d_{C13D\text{-}C18H}$ = 3.585 Å, d_{c5}-c_{18D} = 3.330 Å [c5 (C16H, C17H, C18H, C19H, C20H, C21H)], $d_{C16D\text{-}C16H}$ = 3.396 Å and $d_{c6\text{-}C15H}$ = 3.330 Å [c6 (C16D, C17D, C18D, C19D, C20D, C21D)]. In **13**, π-π-stacking interactions between π clouds of chlorobenzylidene groups of different frameworks are the principal interactions present in the crystal packing, and form antiparallel dimers, $d_{C15J\text{-}c7}$ = 3.502 Å [c7 (C16C-C17C-C18C-C19C-C20C-C21C) and repeated for other centroids] (Figure 13). In **15**,

π-π-stacking interactions between π clouds, of the isopropoxybenzylidene and thiazolidinone groups of different frameworks form antiparallel dimers, d_{c8-c9} = 3.696 Å [c8 (N1J-C6J-S1J-C13J-C14J), c9 (C16A-C17A-C18A-C19A-C20A-C21A) and repeated for other centroids] (Figure 14).

2.3. Biology

2.3.1. Antiamoebic activity

All the hybrid molecules (**3-17**) were evaluated *in vitro* for antiamoebic activity against HM1: IMSS strain of *E. histolytica* by microdilution method [21]. The antiamoebic activity was compared with the standard amoebicidal drug MNZ that had 50% inhibitory concentration (IC_{50}) 1.64 μM. The results manifested that 1-(furan-2-ylmethyl)-3-phenylthiourea (**1**; IC_{50} = 8.22 μM) had higher IC_{50} value than the standard drug. However, compound **2** (IC_{50} = 3.57 μM), which integrates furan and thiazolidinones moieties together in single molecular skeleton had lower IC_{50} value than compound **1**. The compound **1** and compound **2** having different structure were found to exhibit different biological behaviour that suggest that the molecular hybridization of furan and thiazolidinone had an excellent impact on antiamoebic activity. Moreover, Knoevenagel condensation of compound **2** furnished the compounds (**3-17**; IC_{50} = 0.27-2.97 μM) having better antiamoebic potential than compound **2**. Among all the furan-thiazolidinone hybrids, seven compounds (**3, 6, 8, 11, 12, 14** and **16**) exhibited less IC_{50} value than MNZ. Compound **11** (IC_{50} = 0.27 μM) having heterocyclic substituent was found to be endowed with maximum antiamoebic activity. The biological behavior of the compounds revealed that the compound with hydroxyl (**8**, IC_{50} = 1.04 μM), methoxy group (**16**, IC_{50} = 1.35 μM) and methyl (**14**, IC_{50} = 1.48 μM) at *para* position displayed remarkable activity. However, the introduction of nitro (**5**, IC_{50} = 2.87 μM), isopropoxy (**15**, IC_{50} = 2.20 μM), ethoxy (**9**, IC_{50} = 2.03 μM) and chloro (**17**, IC_{50} = 2.33

μM) group at the same position had negative effect on antiamoebic activity. The results suggest that the substituents present on position 5 of thiazolidinone ring play significant role in the activity against HM1: IMSS strain of *E.histolytica*. However, it can be concluded that the entire molecular-skeleton of the particular compound is concerned with its IC_{50} value and therefore, responsible for its antiamoebic activity.

2.3.2. Cytotoxic activity

Cytotoxicity of active compounds has been studied using the MTT cell viability assay on Chinese hamster ovary (CHO) normal cell lines. MTT is a tetrazolium salt, which can be easily reduced to a colored formazan product with the help of reducing enzymes present only in metabolically active or dividing cells [22]. The enzyme succinate dehydrogenase and cytochrome oxidase present in mitochondria of active cells helps in the reduction of MTT [23]. A confluent population of CHO cells was treated with increasing concentrations of compounds and the number of viable cells was measured after 48 h and 72 h by MTT cell viability assay based on mitochondrial reduction of the yellow MTT tetrazolium dye to a highly colored blue formazan product. This assay usually shows high correlation with number of live cells and cell proliferation. The concentration range for all the active compounds (**3, 6, 8, 11, 12, 14, 16** and MNZ) is mentioned in (Figure 15), which illustrates that all the active compounds and metronidazole were least-cytotoxic in the concentration range of 2.5-50 μM for 48 h and 2.5-25 μM for 72 h. At 100 μM for 48 h and 50 μM for 72 h, only three compounds **3, 6** and **11** showed maximum viability and least cytotoxicity respectively (Table 2). Therefore, it can be concluded that the cytotoxicity of all the compounds (**3, 6, 8, 11, 12, 14** and **16**) was found to be concentration-dependent and all the screened compounds were least-cytotoxic against the Chinese hamster ovary (CHO) normal cell lines in the concentration range of 2.5-50 μM.

2.4 Drug –likeness properties

The molecular properties of synthesized compounds with known inhibitors (Table SI3) were analyzed by Lipinski's rule of five. Interestingly all the synthesized compounds and known inhibitors have molecular weight in the range 171– 450 (< 500). Low molecular weight drug molecules (<500) are transported, diffuse and absorbed without difficulty as compared to heavy molecules. Molecular weight is an important aspect in curative drug action; if molecular weight increases from certain limit, the large size of the compounds also increases correspondingly, which in turn affects the drug action [24]. Number of hydrogen bond acceptors (O and N atoms) and number of hydrogen bond donors (NH and OH) in the synthesize compounds and known inhibitors were establish to be within Lipinski's limit range from 4-9 & 0-2 i.e. less than 10 and 5 respectively [25].

2.4.1 Pharmacokinetics and toxicity

Most of drugs fail in clinical trials due to weak pharmacokinetic properties and cellular toxicity. Therefore, *in silico* pharmacokinetic profile of selected compounds was evaluated to fetch the putative bioavailability for *Eh*TrR and *Eh*OASS inhibitors provided in supplementary data (Table SI4). Physicochemical properties, especially aqueous solubility (logS), lipophilicity (clogP), polar surface area (PSA), and molecular weight (MW) are directly related to the absorption and bioavailability of a drug molecule [26]. These properties directly affect the movement of a drug from the site of administration into the blood. The CYPs (cytochrome P450) play a significant role in drug metabolism and are equally important for disposition of drugs in body, their pharmacological and toxicological effects [27]. Here, ADMET (DS3.5) was used to get the probable pharmacokinetic profile of molecules. It utilizes QSAR models to compute the ADMET related properties for small molecules. Alog P value (Lipophilicity) is significant property for the prediction of per oral

bioavailability of drug molecules [24]. Results showed that all virtual synthesized compounds have ideal AlogP value ≤ 5, except synthesized compounds **9, 13, 14, 15** and **17** (logP = 5.226, 5.558, 5.379, 5.603and 5.558 respectively). However, logP value up to 6 is considerable for a drug molecule [28]. Similarly, all hits showed moderate to good range of solubility level (solubility level = 0 to 4). The compound 11 showed better solubility with level 2, AlogP = 3.885, having good absorption (level 0) and moderate hepatotoxicity (level 1). Only one compounds **15** showed hepatotoxicity probability score ≤ 0.5. The observed human intestinal absorption (HIA) value is excellent for all molecules. The blood-brain-barrier (BBB) penetration ability of compounds is high when prediction value is zero and is least for the prediction value of 4. All hybrid molecules showed better ability, except compound **4** and **5** (BBB = 4). The known *Eh*TrR and *Eh*OASS inhibitors, MNZ, 2-{1-[2-(2-methyl-5-nitro-imidazol-1-yl)-ethyl]-*1H*-[1,2,3]triazol-4-yl}-pyridine (A) and 4-hydroxy-2-[2-(1H-indol-3-yl)-2-oxoethyl]sulfanyl- 1H-pyrimidin-6-one (W), are showed good logP value ≤ 5. All have good human intestinal absorption value; however, MNZ and A showed lower probability score of hepatotoxicity, except W higher probability score of hepatotoxicity. The antiamoebic drug MNZ having a good ADMET profile (logP = -0.337, BBB = 3, solubility = 4 and HIA = 0), showed less hepatotoxicity effect and is also not reactive to CYP2D6. All the compounds except **2, 5, 8, 9, 11** and **15** exhibited <0.5 probability value for CYP2D6 enzyme. For good drug ability, the ideal plasma protein binding (PPB) level is 0. All synthesized compounds had > 0 probability PPB activity, whereas MNZ and A showed level-0. PSA is dependent on the conformation and hydrogen-bonding. It implies the single low-energy conformer of the molecule. For activity of a drug, the optimum value of PSA is ≤ 90 Å [29]. The hydrogen bonding and logP value are the important two descriptors to define the PSA of drug molecule. All predicted compounds showed significant PSA, whereas A and W showed higher PSA value ≥ 90 Å. The computer-

aided toxicity predictor, TOPKAT was used to examine the cellular toxicity of synthesize compounds. The carcinogenic and mutagenic effect of compounds with WOE Prediction (weight of evidence) and Ames Prediction was our primary goal. It comprises of various models and toxicity endpoints (irritation, teratogenicity, sensitization, neuro-toxicity and immunotoxicology) that are often employed in drug development. All the selected compounds showed Ames probability score ≤ 7 and are not mutagens except compounds **4** and **5** which has score ≥ 7 and is anticipated as mutagen. All *Eh*TrR and *Eh*OASS inhibitors under study are predicted as non-mutagen, except MNZ and A. Other toxicity predictor WOE was employed to examine the relative level of certainty of compounds that may cause cancer in humans. All compounds were found to be non-carcinogenic, except five virtual compounds (**2, 4, 5, 10** and **11**). MNZ and W are predicted as carcinogenic. The ADMET score and TOPKAT property data of virtual synthesized compounds with standard drug, suggested that selected molecules may be exploited as bioactive compounds.

2.5 Molecular docking

All the title compounds (**3-17**) with reference drug MNZ were targeted for molecular docking studies using rigid docking method. Auto docking 4.2 was used to determine the orientation of inhibitors bound in the active site of the *Eh*TrR and *Eh*OASS protein (4A5L and 3BM5) [30]. The docking of inhibiting ligand molecules **6, 8, 12, 14** and **16** with the protein 4A5L reveals that all the inhibitors are in bonding with more than one amino acid residues except **3, 11**, and **16** and thereby they occupy the active pockets of the protein 4A5L shown in Figure 16 [C, D, E, F, G, H and I]. Theoretically all the seven inhibitor molecules (**3, 6, 8, 11, 12, 14** and **16**) exhibit very good binding energy compared with reference drug MNZ and A as shown in Table 3.

The docking of inhibiting ligand molecules **3, 6, 8, 11, 12, 14** and **16** with the protein 4A5L reveals that all the inhibitors are in bonding with amino acid residues and thereby they occupy the active pockets of the protein 3BM5 shown in Figure 17 [C, D, E, F, G, H and I]. Theoretically all the seven hybrids displayed significant binding energy than the reference drug MNZ and W as shown in Table 4. The inhibitor **3, 6, 8, 12, 14** and **16** formed hydrogen bonds with bond distances range from 2.3 to 3.6 Å with amino acid residues of protein 4A5L and with minimum inhibitory constant as shown in Table 3. Table 4 showed the hydrogen bond distance of inhibitors in the range 3.0 Å - 3.5 Å with amino acid residues of protein 3BM5 and with minimum inhibitory constant. Compounds **3, 6, 8, 11, 12, 14** and **16** were found to have very good binding energy for *Eh*TrR and *Eh*OASS. Therefore, these compounds were good inhibitors of the target protein *Eh*TrR and *Eh*OASS. Among all the docked compounds (**2-17**), only three compounds **3, 6** and **11** showed excellent binding energy for *Eh*TrR and *Eh*OASS, therefore, these may be considered as good inhibitors of proteins (4A5L and 3BM5).

2.6 Enzymatic Inhibition assay

Among all the hybrids, three hybrids (**3, 6** and **11**) with most promising antiamoebic activity were selected for enzymatic inhibition assay against *E. histolytica* O-acetyle-L-serine sulfohydrolase. The enzyme *Eh*OASS was expressed and purified as described previously [31]. Inhibitory kinetics analysis was carried out for *Eh*OASS with varied concentration of furan-thiazolidinone hybrids to measure the decrease in enzymatic activity. The rate of a reaction was found to significantly decrease with increasing concentration of inhibitor. To explore the inhibition of furan-thiazolidinone hybrids, IC_{50} values were calculated by measuring normalized inhibition with increasing log inhibition concentration (Figure 18). Our biochemical experimental results showed that compound **3, 6** and **11** inhibited OASS

with IC_{50} in the range of 137.9-157.5 μM concentration Table 2. Further these molecules could be expected to inhibit thioredoxin reductase and other enzyme in *E. histolytica*.

3. Conclusion

All the synthesized hybrids were capable of inhibiting the growth of *E. histolytica* out of which seven compounds (IC_{50} = 0.27–1.48 μM) were found to have better efficacy than the standard drug MNZ (IC_{50} = 1.64 μM) and the activity was substituent dependent. All the seven hybrids offered remarkable cell viability. Among all hybrids, three compounds (**3, 6** and **11**) showed excellent binding energy for *E. histolytica* O-acetyle-L-serine sulfohydrolase and *E. histolytica* thioredoxin reductase. In summary, three compounds (**3, 6** and **11**) showed most promising antiamoebic activity and significant inhibition of O-acetyle-L-serine sulfohydrolase, therefore these molecules may be subjected to further investigations for the development of novel effective antiamoebic agents.

4. Experimental

All the required chemicals were purchased from Merck and Aldrich Chemical Company (USA). Precoated aluminium sheets (Silica gel 60 F254, Merck Germany) were used for thin-layer chromatography (TLC) and spots were visualized under UV light. The melting points were recorded on Veego instrument with model specifications REC-22038 A2 and are uncorrected. Elemental analyses were performed on Elementar Vario analyzer and the results are within ±0.4% of the theoretical values. IR spectra were acquired at Bruker FT-IR spectrophotometer. ^{1}H and ^{13}C NMR were recorded on a Bruker Spectrospin DPX 400 MHz and Bruker Spectrospin DPX 100 MHz spectrometer respectively, using $CDCl_3$ as a solvent and trimethylsilane (TMS) as the internal standard. Splitting patterns are designated as follows; s, singlet; d, doublet; t, triplet; m, multiplet. Chemical shift values are given in ppm. Mass spectra were recorded by ESI-MS (AB-Sciex 2000, Applied Biosystem).

4.1. General procedure for the synthesis of 1-(furan-2-ylmethyl)-3-phenylthiourea (1)

On treating phenylisothiocyanate (70 mmol) with furfuryl amine (70 mmol) in toluene white precipitates were obtained which were collected by filtration, washed with toluene, and dried to afford 1-(furan-2-ylmethyl)-3-phenylthiourea (**1**).

4.1.1. 1-(Furan-2-ylmethyl)-3-phenylthiourea (1) Yield: 93%; white solid; m.p: 103°C; Anal. calc. (%) for $C_{12}H_{12}N_2OS$: C 62.04, H 5.21, N 12.06, S 13.80. found: C 62.24, H 5.29, N 12.23, S 13.97; FT-IR ν_{max} (cm^{-1}): 3279 (NH), 3059 (C-H, Ar-H), 1238 (C=S); ^{1}HNMR (CDCl3) δ (ppm): 8.36 (s, 1H, NH), 7.43 (t, 2H, *J*=7.60 Hz, Ar-H), 7.33 (s, 1H, S=C-NH), 7.30 (t, 1H, *J*=7.20 Hz, Ar-H), 7.22 (d, 2H, *J*=7.60 Hz, Ar-H), 6.33-6.27 (m, 3H, Ar-H), 4.85 (d, 2H, *J*=5.2 Hz, CH_2); ^{13}C NMR (CDCl3) δ (ppm): 180.46, 150.25, 142.42, 136.01, 130.25, 127.35, 125.12, 110.51, 108.18, 42.34; ESI-MS: m/z = 232.30

4.2. General procedure of synthesis of 3-(furan-2-ylmethyl)-2-(phenylimino)-1, 3-thiazolidin-4-one (2)

1-(Furan-2-ylmethyl)-3-phenylthiourea (30 mmol) was dissolved in ethanol and then anhydrous sodium acetate (60 mmol) and chloroacetic acid (37.5 mmol) were added in the reaction mixture. The suspension was heated under reflux for 12 h and then the solvent was evaporated. Water was added and the aqueous layer was extracted with ethyl acetate. The organic layer was washed with saturated sodium bicarbonate and brine. The combined organic extracts were dried over Na_2SO_4 and concentrated *in vacuo*, consequently yellow solid product 3-(furan-2-ylmethyl)-2-(phenylimino)-1, 3-thiazolidin-4-one (**2**) was obtained.

4.2.1. 3-(Furan-2-ylmethyl)-2-(phenylimino)-1, 3-thiazolidin-4-one (2) Yield: 90%; light brown solid; m.p: 95°C; Anal. calc. (%) for $C_{14}H_{12}N_2O_2S$: C 61.75, H 4.44, N 10.29, S 11.77. found: C 61.54, H 4.62, N 10.11, S 11.52; FT-IR ν_{max} (cm^{-1}): 1723 (-N-C=O), 1620 (C=N),

1376 (tert. N), 754 (C-S-C); ^{1}H NMR (CDCl3) δ (ppm): 7.38-7.33 (m, 3H, Ar-H), 7.17 (t, 1H, *J*=7.6 Hz, Ar-H), 6.98 (d, 2H, *J*=7.2, Ar-H), 6.43 (d, 1H, Ar-H), 6.35-6.33 (m, 1H, Ar-H), 5.04 (s, 2H, CH_2), 3.81 (s, 2H, CH_2); ^{13}C NMR ($CDCl_3$) δ (ppm): 171.31, 153.40, 149.09, 147.86, 142.37, 129.28, 124.70, 121.01, 110.50, 109.60, 39.06, 32.68; ESI-MS: m/z = 272.32.

4.3. General procedure of synthesis of Furan-thiazolidinone hybrids (3-17)

A mixture of 3-(Furan-2-ylmethyl)-2-(phenylimino)-1, 3-thiazolidin-4-one (1 mmol), different aldehydes (1 mmol), hexahydropyridine (1.15 mmol), and ethanol (35 mL) were heated under reflux for 11-12 h. The reaction mixture was cooled to room temperature and the precipitates were obtained which were filtered, washed and recrystallized from ethanol to furnished final products (**3-17**).

4.3.1. 5-(3, 4-Dimethoxybenzylidene)-3-(furan-2-ylmethyl)-2-(phenylimino)-1, 3-thiazolidin-4-one (3) Yield: 83%; yellow solid; m.p. 126°C; Anal. Calc. $C_{23}H_{20}N_2O_4S$: C 65.70, H 4.79, N 6.66, S 7.63%. found: C 65.52, H 4.63, N 6.42, S 7.55%; FT-IR ν_{max} (cm^{-1}): 1710 (-N-C=O), 1643 (C=N), 1594 (C=C), 1374 (tert. N), 760 (C-S-C); ^{1}H NMR ($CDCl_3$) δ (ppm): 7.70 (s, 1H, =CH), 7.38 (t, 3H, *J*=7.6 Hz, Ar-H), 7.18 (t, 1H, *J*=7.6, Ar-H), 7.05-7.02 (m, 1H, Ar-H), 7.01 (d, 2H, *J*=7.2 Hz, Ar-H), 6.91 (s, 1H, Ar-H), 6.87 (d, 1H, *J*=8.4 Hz, Ar-H), 6.43 (s, 1H, Ar-H), 6.32-6.31 (m, 1H, Ar-H), 5.15 (s, 2H, CH_2), 3.87 (s, 3H, OCH_3), 3.83 (s, 3H, OCH_3); ^{13}C NMR ($CDCl_3$) δ (ppm): 166.49, 149.69, 149.21, 149.11, 148.05, 142.39, 131.33, 129.33, 126.67, 124.88, 123.42, 121.24, 118.95, 113.06, 111.26, 110.48, 109.49, 55.99, 39.06; ESI-MS: m/z = 420.48.

4.3.2. 5-(3-Nitrobenzylidene) - 3-(furan-2-ylmethyl)-2-(phenylimino)-1, 3-thiazolidin-4-one (4) Yield: 85%; off white solid; m.p. 153°C; Anal. Calc. $C_{21}H_{15}N_3O_4S$: C 62.21, H 3.73, N 10.36, S 7.91%. found: C 62.49, H 3.85, N 10.57, S 7.64 %; FT-IR ν_{max} (cm^{-1}): 1710 (-N-

C=O), 1639 (C=N), 1595 (C=C), 1340 (tert. N), 767 (C-S-C); ^{1}H NMR ($CDCl_3$) δ (ppm): 8.27 (s, 1H, Ar-H), 8.20 (d, 1H, *J*=7.6 Hz, Ar-H), 7.80 (s, 1H, =CH), 7.74 (d, 1H, *J*=7.6 Hz, Ar-H), 7.61 (t, 1H, *J*=8.0 Hz, Ar-H), 7.43-7.40 (m, 3H, Ar-H), 7.24 (t, 1H, *J*=7.6 Hz, Ar-H), 7.02 (d, 2H, *J*=7.6 Hz, Ar-H), 6.48 (s, 1H, Ar-H), 6.36 (s, 1H, Ar-H), 5.20 (s, 2H, CH_2); ^{13}C NMR ($CDCl_3$) δ (ppm): 165.69, 148.81, 148.67, 148.14, 147.55, 142.54, 135.47, 134.63, 130.07, 129.48, 128.01, 125.30, 125.18, 124.48, 123.90, 121.02, 110.52, 109.75, 39.39; ESI-MS: m/z = 405.42.

4.3.3. 5-(4-Nitrobenzylidene) - 3-(furan-2-ylmethyl)-2-(phenylimino)-1, 3-thiazolidin-4-one (5) Yield: 83%; yellow solid; m.p. 228°C; Anal. Calc. $C_{21}H_{15}N_3O_4S$: C 62.21, H 3.73, N 10.36, S 7.91%. found: C 62.32, H 3.77, N 10.21, S 7.96 %; FT-IR ν_{max} (cm^{-1}): 1704 (-N-C=O), 1637 (C=N), 1590 (C=C), 1372 (tert. N), 756 (C-S-C); ^{1}H NMR ($CDCl_3$) δ (ppm): 8.25 (d, 2H, *J*=8.4 Hz, Ar-H), 7.79 (s, 1H, =CH), 7.59 (d, 2H, *J*=8.4 Hz, Ar-H), 7.43-7.40 (m, 3H, Ar-H), 7.25-7.22 (m, 1H, Ar-H), 7.02 (d, 2H, *J*=7.2 Hz, Ar-H), 6.48 (s, 1H, Ar-H), 6.36 (s, 1H, Ar-H), 5.23 (s, 2H, CH_2); ^{13}C NMR ($CDCl_3$) δ (ppm): 165.67, 148.73, 148.20, 147.60, 142.58, 139.86, 130.33, 129.49, 127.93, 126.28, 125.34, 124.21, 121.03, 110.54, 109.82, 39.40; ESI-MS: m/z = 405.42

4.3.4. 5-(2, 5-Dimethoxybenzylidene)-3-(furan-2-ylmethyl)-2-(phenylimino)-1, 3-thiazolidin-4-one (6) Yield: 83%; yellow solid; m.p. 99°C; Anal. Calc. $C_{23}H_{20}N_2O_4S$: C 65.70, H 4.79, N 6.66, S 7.63%. found: C 65.61, H 4.57, N 6.33, S 7.74 %; FT-IR ν_{max} (cm^{-1}): 1710 (-N-C=O), 1633 (C=N), 1588 (C=C), 1360 (tert. N), 750 (C-S-C); ^{1}H NMR ($CDCl_3$) δ (ppm): 8.13 (s, 1H, =CH), 7.38-7.35 (m, 3H, Ar-H), 7.19 (t, 1H, *J*=7.2 Hz, Ar-H), 7.01 (d, 2H, *J*=7.6 Hz, Ar-H), 6.90 (s, 1H, Ar-H), 6.86-6.81 (m, 2H, Ar-H), 6.45 (s, 1H, Ar-H), 6.34 (s, 1H, Ar-H), 5.18 (s, 2H, -CH_2), 3.81 (s, 3H, OCH_3), 3.72 (s, 3H, OCH_3); ^{13}C NMR ($CDCl_3$) δ (ppm): 166.26, 153.38, 152.81, 149.72, 149.29, 147.96, 142.32, 129.29, 126.58,

124.82, 123.67, 121.88, 121.19, 116.02, 114.61, 112.02, 110.45, 109.42, 56.08, 55.81, 39.03; ESI-MS: m/z = 420.48

4.3.5. 5-(1, 3-Benzodioxol-5-ylmethylidene)-3-(furan-2-ylmethyl)-2-(phenylimino)-1, 3-thiazolidin-4-one (7) Yield: 85%; yellow solid; m.p. 130°C; Anal. Calc. $C_{22}H_{16}N_2O_4S$: C 65.33, H 3.99, N 6.93, S 7.93%. found: C 65.61, H 4.15, N 7.21, S 8.19 %; FT-IR ν_{max} (cm^{-1}): 1701 (-N-C=O), 1641 (C=N), 1583 (C=C), 1365 (tert. N), 744 (C-S-C); ^{1}H NMR ($CDCl_3$) δ (ppm): 7.68 (s, 1H, =CH), 7.41-7.38 (m, 3H, Ar-H), 7.20 (t, 1H, *J*=7.2 Hz, Ar-H), 7.02-6.97 (m, 3H, Ar-H), 6.92 (s, 1H, Ar-H), 6.84 (d, 1H, *J*=8.0 Hz, Ar-H), 6.46 (s, 1H, Ar-H), 6.35 (s, 1H, Ar-H), 6.00 (s, 2H, OCH_2), 5.17 (s, 2H, CH_2); ^{13}C NMR ($CDCl_3$) δ (ppm): 166.44, 149.54, 149.22, 149.11, 148.33, 148.07, 142.36, 131.14, 129.38, 128.01, 125.99, 124.90, 121.19, 119.18, 110.46, 109.46, 109.08, 108.93, 101.72, 39.09; ESI-MS: m/z = 404.43

4.3.6. 5-(4-Hydroxybenzylidene) - 3-(furan-2-ylmethyl)-2-(phenylimino)-1, 3-thiazolidin-4-one (8) Yield: 83%; brown solid; m.p. 153°C; Anal. Calc. $C_{21}H_{16}N_2O_3S$: C 67.00, H 4.28, N 7.44, S 8.52%. found: C 65.26, H 4.41, N 7.66, S 8.59 %; FT-IR ν_{max} (cm^{-1}): 1700 (-N-C=O), 1626 (C=N), 1577 (C=C), 1369 (tert. N), 761 (C-S-C); ^{1}H NMR ($CDCl_3$) δ (ppm): 7.71 (s, 1H, =CH), 7.41-7.37 (m, 3H, Ar-H), 7.31 (d, 2H, *J*=8.4 Hz, Ar-H), 7.21 (t, 1H, *J*=7.6 Hz, Ar-H), 7.03 (d, 2H, *J*=7.6 Hz, Ar-H), 6.81 (d, 2H, *J*=8.8 Hz, Ar-H), 6.44 (s, 1H, Ar-H), 6.37 (bs, 1H, OH), 6.33 (s, 1H, Ar-H), 5.17 (s, 2H, CH_2); ^{13}C NMR ($CDCl_3$) δ (ppm): 166.88, 159.73, 150.12, 149.28, 148.22, 142.32, 132.32, 131.82, 129.34, 124.98, 124.78, 121.26, 117.15, 116.66, 110.46, 109.37, 39.40; ESI-MS: m/z = 376.42.

4.3.7. 5-(4-Ethoxylbenzylidene) - 3-(furan-2-ylmethyl)-2-(phenylimino)-1, 3-thiazolidin-4-one (9) Yield: 84%; off white solid; m.p. 107°C; Anal. Calc. $C_{23}H_{20}N_2O_3S$: C 68.30, H 4.98, N 6.93, S 7.93%. found: C 68.53, H 4.87, N 6.78, S 7.74%; FT-IR ν_{max} (cm^{-1}): 1706 (-N-C=O), 1635 (C=N), 1588 (C=C), 1373 (tert. N), 741 (C-S-C); ^{1}H NMR ($CDCl_3$) δ (ppm):

7.74 (s, 1H, =CH), 7.42-7.37 (m, 5H, Ar-H), 7.22 (t, 1H, *J*=7.6 Hz, Ar-H), 7.03 (d, 2H, *J*=7.2 Hz, Ar-H), 6.91 (d, 2H, *J*=8.8 Hz, Ar-H), 6.46 (s, 1H, Ar-H), 6.35 (s, 1H, Ar-H), 5.18 (s, 2H, CH_2), 4.07 (m, 2H, CH_2), 1.44 (t, 3H, *J*=7.2, CH_3); ^{13}C NMR ($CDCl_3$) δ (ppm): 166.60, 160.32, 149.88, 149.29, 148.21, 142.34, 131.91, 131.23, 129.35, 126.17, 124.81, 121.25, 118.28, 115.02, 110.46, 109.42, 63.68, 39.04, 14.69; ESI-MS: m/z = 404.48

4.3.8. 5-Benzylidene-3-(furan-2-ylmethyl)-2-(phenylimino)-1, 3-thiazolidin-4-one (10) Yield: 83%; dark yellow solid; m.p. 120°C; Anal. Calc. $C_{21}H_{15}N_3O_3S$: C 69.98, H 4.47, N 7.77, S 8.90%. found: C 69.71, H 4.64, N 7.71, S 8.54 %; FT-IR ν_{max} (cm^{-1}): 1711 (-N-C=O), 1631 (C=N), 1586 (C=C), 1371 (tert. N), 727 (C-S-C); ^{1}H NMR ($CDCl_3$) δ (ppm): 7.79 (s, 1H, =CH), 7.45-7.33 (m, 8H, Ar-H), 7.29 (t, 1H, *J*=7.6 Hz, Ar-H), 7.03 (d, 2H, *J*=7.6 Hz, Ar-H), 6.47 (s, 1H, Ar-H), 6.36 (s, 1H, Ar-H), 5.19 (s, 2H, -CH_2); ^{13}C NMR ($CDCl_3$) δ (ppm): 166.31, 149.52, 149.18, 148.03, 142.38, 133.74, 131.24, 129.95, 129.79, 129.36, 129.01, 124.91, 121.51, 121.19, 110.47, 109.47, 39.14; ESI-MS: m/z = 360.42

4.3.9. 5-(Pyridin-2-ylmethylidene)-3-(furan-2-ylmethyl)-2-(phenylimino) - 1, 3-thiazolidin-4-one (11) Yield: 83%; yellow solid; m.p. 196°C; Anal. Calc. $C_{20}H_{15}N_3O_2S$: C 66.46, H 4.18, N 11.63, S 8.87%. found: C 66.33, H 4.37, N 11.54, S 8.56 %; FT-IR ν_{max} (cm^{-1}): 1705 (-N-C=O), 1635 (C=N), 1581 (C=C), 1373 (tert. N), 750 (C-S-C); ^{1}H NMR ($CDCl_3$) δ (ppm): 8.61 (s, 1H, Ar-H), 7.67 (s, 1H, =CH), 7.65 (m, 1H, Ar-H), 7.42 (d, 1H, *J*=8.0 Hz, Ar-H), 7.39-7.35 (m, 3H, Ar-H), 7.18-7.13 (m, 2H, Ar-H), 7.03 (d, 2H, *J*=7.2 Hz, Ar-H), 6.43-6.42 (m, 1H, Ar-H), 6.32-6.31 (m, 1H, Ar-H), 5.16 (s, 2H, CH_2); ^{13}C NMR ($CDCl_3$) δ (ppm): 166.48, 153.12, 152.28, 149.31, 149.29, 147.93, 142.34, 136.72, 129.31, 126.98, 126.78, 126.63, 124.63, 122.85, 121.32, 110.49, 109.37, 38.52; ESI-MS: m/z = 361.41.

4.3.10. 5-(3, 4, 5-Trimethoxybenzylidene)-3-(furan-2-ylmethyl)-2-(phenylimino)-1, 3-thiazolidin-4-one (12) Yield: 83%; off white solid; m.p. 102°C; Anal. Calc. $C_{24}H_{22}N_2O_5S$: C

63.98, H 4.92, N 6.22, S 7.12%. found: C 63.91, H 4.85, N 6.44, S 7.31 %; FT-IR ν_{max} (cm^{-1}): 1710 (-N-C=O), 1641 (C=N), 1593 (C=C), 1372 (tert. N), 759 (C-S-C); ^{1}H NMR ($CDCl_3$) δ (ppm): 7.67 (s, 1H, =CH), 7.36-7.32 (m, 3H, Ar-H), 7.16 (d, 1H, *J*=7.2 Hz, Ar-H), 7.00 (d, 2H, *J*=7.6 Hz, Ar-H), 6.63 (s, 2H, Ar-H), 6.43 (s, 1H, Ar-H), 6.32 (s, 1H, Ar-H), 5.15 (s, 2H, -CH_2), 3.84 (s, 3H, OCH_3), 3.79 (s, 6H, OCH_3); ^{13}C NMR ($CDCl_3$) δ (ppm): 166.19, 153.49,149.18, 147.83, 142.36, 139.95, 139.92, 131.34, 129.26, 124.94, 121.17, 120.69, 110.46, 109.44, 107.49, 107.47, 60.93, 56.30, 39.14; ESI-MS: m/z = 450.50.

4.3.11. 5-(3-Chlorobenzylidene) - 3-(furan-2-ylmethyl)-2-(phenylimino)-1, 3-thiazolidin-4-one (13) Yield: 83%; yellow solid; m.p. 103°C; Anal. Calc. $C_{21}H_{15}N_2O_2SCl$: C 63.87, H 3.83, N 7.09, S 8.12%. found: C 63.61, H 3.57, N 7.25, S 8.47 %; FT-IR ν_{max} (cm^{-1}): 1712 (-N-C=O), 1636 (C=N), 1589 (C=C), 1371 (tert. N), 754 (C-S-C); ^{1}H NMR ($CDCl_3$) δ (ppm): 7.70 (s, 1H, =CH), 7.43-7.39 (m, 4H, Ar-H), 7.32 (s, 3H, Ar-H), 7.23 (t, 1H, *J*=7.2 Hz, Ar-H), 7.03 (d, 2H, *J*=7.2 Hz, Ar-H), 6.47-6.46 (m, 1H, Ar-H), 6.36-6.35 (m, 1H, Ar-H), 5.19 (s, 2H, CH_2); ^{13}C NMR ($CDCl_3$) δ (ppm): 166.00, 149.00, 148.83, 147.77, 142.46, 135.50, 135.07, 130.22, 129.77, 129.70, 129.48, 129.43, 127.60, 125.09, 123.20, 121.11, 110.50, 109.62, 39.25; ESI-MS: m/z = 394.87

4.3.12. 5-(4-Methylbenzylidene) - 3-(furan-2-ylmethyl)-2-(phenylimino)-1, 3-thiazolidin-4-one (14) Yield: 87%; pale yellow solid; m.p.121°C; Anal. Calc. $C_{22}H_{18}N_2O_2S$: C 70.57, H 4.85, N 7.48, S 8.56%. found: C 70.32, H 4.81, N 7.33, S 8.27 %; FT-IR ν_{max} (cm^{-1}): 1708 (-N-C=O), 1639 (C=N), 1593 (C=C), 1361 (tert. N), 755 (C-S-C); ^{1}H NMR ($CDCl_3$) δ (ppm): 7.77 (s, 1H, =CH), 7.42-7.38 (m, 3H, Ar-H), 7.35 (d, 2H, *J*=8.0 Hz, Ar-H), 7.21 (d, 3H, 8.0 Hz, Ar-H), 7.04 (d, 2H, *J*=7.6 Hz, Ar-H), 6.46 (m, 1H, Ar-H), 6.36-6.34 (m, 1H, Ar-H), 5.19 (s, 2H, -CH_2), 2.36 (s, 3H, CH_3); ^{13}C NMR ($CDCl_3$) δ (ppm): 166.46, 149.72, 149.23,148.10 ,142.36 ,140.41, 131.38, 130.96, 130.03, 129.77, 129.35, 124.86, 121.22, 120.24, 110.46, 109.45, 39.08, 21.51; ESI-MS: m/z = 374.45

4.3.13. 5-(4-Isopropoxybenzylidene) - 3-(furan-2-ylmethyl)-2-(phenylimino)-1, 3-thiazolidin-4-one (15) Yield: 83%; yellow solid; m.p. 103°C; Anal. Calc. $C_{24}H_{22}N_2O_3S$: C 68.88, H 5.30, N 6.69, S 7.66%. found: C 68.61, H 5.37, N 6.61, S 7.47 %; FT-IR ν_{max} (cm^{-1}): 1708 (-N-C=O), 1636 (C=N), 1594 (C=C), 1375 (tert. N), 770 (C-S-C); ^{1}H NMR ($CDCl_3$) δ (ppm): 7.71 (s, 1H, =CH), 7.39-7.34 (m, 5H, Ar-H), 7.19 (t, 1H, *J*=7.6 Hz, Ar-H), 7.01 (d, 2H, *J*=8.0 Hz, Ar-H), 6.87 (d, 2H, *J*=8.8 Hz, Ar-H), 6.44 (s, 1H, Ar-H), 6.33 (s, 1H, Ar-H), 5.16 (s, 2H, CH_2), 4.58-4.52 (m, 1H, CH), 1.32 (d, 6H, *J*=6.0 Hz, CH_3); ^{13}C NMR ($CDCl_3$) δ (ppm): 166.66, 159.39, 149.96, 149.28, 148.20, 142.37, 131.97, 131.30, 129.36, 125.91, 124.82, 121.26, 118.11, 116.01, 110.48, 109.45, 70.08, 39.04, 21.94; ESI-MS: m/z = 418.50

4.3.14. 5-(4-Methoxybenzylidene) - 3-(furan-2-ylmethyl)-2-(phenylimino)-1, 3-thiazolidin-4-one (16) Yield: 83%; yellow solid; m.p. 135°C; Anal. Calc. $C_{22}H_{18}N_2O_3S$: C 67.67, H 4.65, N 7.17, S 8.21%. found: C 67.39, H 4.32, N 6.94, S 8.31 %; FT-IR ν_{max} (cm^{-1}): 1706 (-N-C=O), 1633 (C=N), 1586 (C=C), 1368 (tert. N), 743 (C-S-C); ^{1}H NMR ($CDCl_3$) δ (ppm): 7.74 (s, 1H, =CH), 7.40-7.39 (m, 5H, Ar-H), 7.21 (t, 1H, *J*=7.6 Hz, Ar-H), 7.04 (d, 2H, *J*=7.2 Hz, Ar-H), 6.92 (d, 2H, *J*=8.4 Hz, Ar-H), 6.46 (s, 1H, Ar-H), 6.35 (s, 1H, Ar-H), 5.18 (s, 2H, CH_2), 3.82 (s, 3H, OCH_3); ^{13}C NMR ($CDCl_3$) δ (ppm): 166.54, 160.90, 149.81, 149.31, 148.20, 142.33, 131.87, 131.11, 129.34, 126.40, 124.82, 121.24, 118.54, 114.57, 110.46, 109.40, 55.39, 39.06; ESI-MS: m/z = 390.45

4.3.15. 5-(4-Chlorobenzylidene) - 3-(furan-2-ylmethyl)-2-(phenylimino)-1, 3-thiazolidin-4-one (17) Yield: 85%; off white solid; m.p: 113°C; Anal. Calc. $C_{21}H_{15}N_2O_2SCl$: C 63.87, H 3.83, N 7.09, S 8.12%. found: C 63.96, H 4.01, N 7.26, S 8.17 %; FT-IR ν_{max} (cm^{-1}): 1712 (-N-C=O), 1646 (C=N), 1593 (C=C), 1377 (tert. N), 733 (C-S-C); ^{1}H NMR ($CDCl_3$) δ (ppm): 7.72 (s, 1H, =CH), 7.43-7.39 (m, 3H, Ar-H), 7.36 (s, 4H, Ar-H), 7.23 (t, 1H, *J*=7.2 Hz, Ar-H), 7.03 (d, 2H, *J*=7.6 Hz, Ar-H), 6.47 (m, 1H, Ar-H), 6.35 (s, 1H, Ar-H), 5.19 (s, 2H, -CH_2); ^{13}C NMR ($CDCl_3$) δ (ppm): 166.17, 149.10, 149.02, 147.91, 142.48, 135.81, 132.16, 131.08,

129.75, 129.43, 129.33, 125.06, 122.10, 121.15, 110.52, 109.65, 39.19; ESI-MS: m/z = 394.87

5. X-Ray crystal structure determination

Three-dimensional X-ray data were collected on a Bruker Kappa Apex CCD diffractometer at low temperature for 2, 6, 8, 13 and 15 by the ϕ-ω scan method. Reflections were measured from a hemisphere of data collected from frames, each of them covering 0.3º in ω. A total of 45012 for 2, 56226 for 6, 98155 for 8, 60473 for 13 and 28530 for 15 reflections measured were corrected for Lorentz and polarization effects and for absorption by multi-scan methods based on symmetry-equivalent and repeated reflections. Of the total, 3592 for 2, 4254 for 6, 5450 for 8, 5121 for 13 and 3681 for 15, independent reflections exceeded the significance level ($|F|/\sigma|F|$) > 4.0, respectively. After data collection, in each case an empirical absorption correction (SADABS) [32] was applied, and the structures were solved by direct methods and refined by full matrix least-squares on F^2 data using SHELX suite of programs [33]. In 2, 13 and 15 hydrogen atoms were located in difference Fourier map and left to refine freely. In 6, hydrogen atoms were located in difference Fourier map and left to refine freely, except for C(22) and C(23), which were included in calculation position and refined in the riding mode. In 8, hydrogen atoms were located in difference Fourier map and left to refine freely, except for O(3), C(4S) and O(6), which were included in calculation position and refined in the riding mode. Refinements were done with allowance for thermal anisotropy of all non-hydrogen atoms. A final difference Fourier map showed no residual density outside: 0.415 and -0.215 e.Å^{-3} for 2, 0.343 and -0.287 e.Å^{-3} for 6, 0.657 and -0.584 e.Å^{-3} for 8, 0.689 and -0.577 e.Å^{-3} for 13 and 0.533 and -0.344 e.Å^{-3} for 15. A weighting scheme w = $1/[\sigma^2(F_o^2) + (0.048200\ P)^2 + 0.388800\ P]$ for 2, w = $1/[\sigma^2(F_o^2) + (0.043600\ P)^2 + 0.630100\ P]$ for 6, w = $1/[\sigma^2(F_o^2) + (0.057000\ P)^2 + 3.064500\ P]$ for 8, w = $1/[\sigma^2(F_o^2) + (0.054700\ P)^2$

+ 0.500400 P] for 13 and w = $1/[\sigma^2(F_o^2) + (0.067300\ P)^2 + 0.191600\ P]$ for 15, where P = $(|F_o|^2 + 2|F_c|^2)/3$, were used in the latter stages of refinement. Further details of the crystal structure determination are given in Table 1. CCDC 1472093-1472097 contain the supplementary crystallographic data for the structures reported in this paper. These data can be obtained free of charge via http://www.ccdc.cam.ac.uk/conts/retrieving.html, or from the Cambridge Crystallographic Data Centre, 12 Union Road, Cambridge CB2 1EZ, UK; fax: (+44) 1223 336 033; or e-mail: deposit@ccdc.cam.ac.uk. Supplementary data associated with this article can be found, in the online version, at doi: $$$$$.

6. Pharmacological Evaluation

6.1. Antiamoebic activity

All the desired compounds (1-17) were screened for *in vitro* antiamoebic activity against HM1: IMSS strain of *E. histolytica* by microdilution method [21]. *E. histolytica* trophozoites were cultured in culture tubes by using Diamond TYIS-33 growth medium [34]. The test compounds (1mg) were dissolved in DMSO (40 µL, level at which no inhibition of amoeba occurs) [35]. The stock solutions of the compounds were prepared freshly before use at a concentration of 1 mg/mL. Two-fold serial dilutions were made in the wells of 96-well microtiter plate (costar). Each test includes metronidazole as a standard amoebicidal drug, control wells (culture medium plus amoebae) and a blank (culture medium only). All the experiments were carried out in triplicate at each concentration level and repeated thrice. The amoeba suspension was prepared from a confluent culture by pouring off the medium at 37 °C and adding 5 mL of fresh medium, chilling the culture tube on ice to detach the organisms from the side of flask. The number of amoeba/mL was estimated with the help of a haemocytometer, using trypan blue exclusion to confirm the viability. The suspension was diluted to10^5 organism/mL by adding fresh medium and 170 µL of this suspension was added

to the test and control wells in the plate so that the wells were completely filled (total volume, 340 mL). An inoculum of 1.7 x 10^4 organisms/well was chosen so that confluent, but not excessive growth, took place in control wells. Plate was sealed and gassed for 10 min with nitrogen before incubation at 37 °C for 72 h. After incubation, the growth of amoeba in the plate was checked with a low power microscope. The culture medium was removed by inverting the plate and shaking gently. Plate was then immediately washed with sodium chloride solution (0.9%) at 37 °C. This procedure was completed quickly and the plate was not allowed to cool in order to prevent the detachment of amoeba. The plate was allowed to dry at room temperature and the amoebae were fixed with methanol and when dried, stained with (0.5%) aqueous eosin for 15 min. The stained plate was washed once with tap water, then twice with distilled water and then allowed to dry. A 200 µL portion of 0.1 N sodium hydroxide solutions was added to each well to dissolve the protein and release the dye. The optical density of the resulting solution in each well was determined at 490 nm with a microplate reader. The % inhibition of amoebal growth was calculated from the optical densities of the control and test wells and plotted against the logarithm of the dose of the drug tested. Linear regression analysis was used to determine the best fitting line from which the IC_{50} value was found. The IC_{50} values are reported in Table 2.

6.2 Toxicity assays

6.2.1. Cell viability (MTT) assay:

The Chinese hamster ovary (CHO) cells were obtained from NCCS (Pune, India). The cells were cultured in Roswell Park Memorial Institute (RPMI) (Sigma Aldrich) with 10% foetal bovine serum (Gibco-life technologies) and 1% penicillin-streptomycin-neomycin. The effect of compounds **3, 6, 8, 11, 12, 14, 16** and the standard drug MNZ on cell proliferation was measured by using an MTT-based assay [23]. Briefly, the cells (5,000/well) were incubated

in triplicate in a 96-well plate in the presence of various concentrations of compounds **3, 6, 8, 11, 12, 14, 16** as well as MNZ or vehicle DMSO (dimethyl sulphoxide) alone in a final volume of 100 µL at 37 ^{0}C and 5% CO_2 in and humidified atmosphere chamber for 48 h and 72 h. At the end of this time period, 20 µL of MTT solution (5 mg/mL in PBS) was added to each well, and the cells were incubated at 37^{0}C in a humidified atmosphere chamber for 4 h. After 4 h, the supernatant was removed from each well. The colored formazan crystal produced from MTT was dissolved in 100 µL of DMSO, and then the absorbance value was measured at 570 nm by a multi-scanner auto reader (Bio-Rad). The following formula was used for the calculation of the percentage of cell viability [36]:

CV= (absorbance of the experimental samples/ absorbance of the control sample) x 100

6.3 In silico pharmacokinetics analysis

6.3.1. Measuring drug -likeness

Drug like properties of compounds were analyzed by the online tool Molinspiration server (http://www.molinspiration.com). A Molinspiration support for calculation of important molecular properties is based on Lipinski Rules of five such as (molecular weight, number of hydrogen bond donors and acceptors) [25].

6.3.2. ADMET Predictions

Discovery studio 3.5 (Accelrys San Diego, USA) was used to generate ADMET values. The Absorption, Distribution, Metabolism, Excretion and Toxicity commonly abbreviated as ADMET properties are considered before designing a drug as these properties plays an important role in clinical phases. Administration of these properties before drug designing leads to cost savings in drug design [37]. These studies resulted in identification of antiamoebic compounds. The after effects of drug intake are administered by TOPKAT. It

assesses the toxicological endpoints by Quantitative Structure Toxicity Relationship (QSTR). Ames mutagen predication, Ames probability, Ames enrichment and weight of evidence are tested by toxicity profile of the compounds.

6.3.3. Preparation of ligands

The structures of ligands were drawn by using Chemdraw ultra 8.0. The structure of ligand was copied in a smile form and then translated using online smile translator (http://cactus.nci.nih.gov/translate/). The PDB file of ligand was then generated and this PDB file was converted into PDBQT file by such process like (detect root, chose the torsion and set the number of torsion) with using Auto Dock Tools (ADT) version 1.5.6 from the Scripps Research Institute.

6.3.4. Selection and preparation of target protein

The crystal structure of *E. histolytica* thioredoxin reductase (*Eh*TrR) and *E. histolytica* O-acetyl serine sulfhydrylase (*Eh*OASS) were selected as a drug target. Its structure (PDB ID: 4A5L and 3BM5) has been retrieved from RCSB protein Data Bank. All water molecules were removed and on the final stage hydrogen atoms were added to the target protein molecule. Then PDB file was converted into PDBQT file by using Auto Dock Tools (ADT) version 1.5.6 from the Scripps Research Institute.

6.3.5. Molecular docking

Molecular docking stimulation using the ligand molecules with *Eh*TrR (PDB ID: 4A5L) and *Eh*OASS (PDB ID: 3BM5) were conducted using Autodock 4.2 docking suite by employing Lamarckian genetic algorithm [30]. The ligands were set to explore and flexible to rotate most probable binding poses, while receptor was kept rigid. The grid maps representing the center of active site pocket for the ligand were calculated with Autogrid. The dimensions of

the grid for *Eh*TrR and *Eh*OASS were 64 × 64 × 64 grid points with aspacing of 0.575 Å between the grid points but centered on the ligand for both receptor (-6.670, 3.419 and -14.903 coordinates and -5.500, 26.609 and 0.418 coordinates). In the present docking study was performed by each run with population of 150 individuals, rate of gene mutation 0.02, cross-over rate 0.8 and the remaining parameters were set as default. Ten poses docking conformations were generated and the best docked conformation was selected based on the Autodock binding energy (Kcal/mol), for further analysis. Finally, the results generated were visualized by PyMOL viewer for analysis minimum binding energy (Kcal/mol), Ki (Inhibition constant) value (μM), and hydrogen and hydrophobic interaction of the docked inhibitor to the modeled structure.

6.5 Enzymatic Inhibition Assay

The sulfhydrylase activity was monitored using TNB (5-thio-2-nitrobenzoate) as an alternative substrate as described previously [38]. O-acetyl L-serine (OAS), 5, 5'-Dithiobis-(2-Nitrobenzoic Acid) (DTNB) and HEPES buffer were purchased from sigma. The disappearance (decrease in color of TNB as it was utilized in reaction) of TNB was measured continuously with increasing concentration of Inhibitor at 412 nm using Uv-visible spectrophotometer (GE Healthcare). A typical assay contained 100mM HEPES pH 7.0, 50 mM TNB, 90 μg *Eh*OASS and inhibitor concentration was varied from 0.25 to 500 μM. This reaction mixture was incubated at room temperature for 30 min. The reaction was started by the addition of substrate OAS and a decrease in enzyme activity is monitored over a fixed interval of time in the presence of varied concentrations of inhibitor. The pattern of the standard reaction is compared with the ones with the inhibitor and percentage decrease in activity calculated using the equation:

100 − ((decrease in absorbance for reactions with inhibitor/decrease in absorbance for standard reaction) × 100) [39].

To determine the IC_{50} for inhibitors, its concentration was varied from 0.25 to 500 μM, while keeping the OASS concentration constant at 20 μM.

Acknowledgement

One of the authors MFA is thankful to University Grant Commission, India for providing BSR meritorious fellowship.

References

[1] A. Debnath, D. Parsonage, R. M. Andrade, C. He, E. R. Cobo, K. Hirata, S. Chen, G. Garcia-Rivera, E. Orozco, M. B. Martinez, S. S. Gunatilleke, A. M. Barrios, M. R. Arkin, L. B. Poole, J. H. McKerrow, S. L. Reed, *Nat. Med.*, 2012, 18, 956.

[2] R. K. Ralston, *Curr. Opin. Microbiol*., 2015, 12, 26.

[3] K. S. Ralston, W. A. Petri, *Essays Biochem,* 2011, 91, 193.

[4] C. Shimokawa, R. Culleton, T. Imai, K. Suzue, M. Hirai, T. Taniguchi, S. Kobayashi, H. Hisaeda, S. Harano, *PLoS One,* 2013, 8, e82025.

[5] A. F. El-Nahas, I. M. El-Ashmawy, *Basic Clin. Pharmacol. Toxicol.*, 2004, 94, 226.

[6] V. Purohit, K. A. Basu, *Chem. Res. Toxicol.,* 2000, 13, 673.

[7] S. Backer, P. Hoffman, E. R. Houpt, *Am. J. Trop. Med. Hyg.*, 2011, 84, 581.

[8] R. C. Fahey, G. L. Newton, B. Arrick, T. Overdank-Bogart, S. B. Aley, *Science*, 1984,

224, 70.

[9] D. G. Arias, E. L. Regner, A. A. Iglesias, S. A. Guerrero, *Biochim. Biophys. Acta Gen. Subj.*, 2012, 1820, 1859.

[10] A. Holmgren, C. Johansson, C. Berndt, M. E. Lonn, C. Hudemann, C. H. Lillig, *Biochem. Soc. Trans.*, 2005, 33, 1375.

[11] T. Jaeger, L. Flohe, *Biofactors*, 2006, 27, 109.

[12] D. Leitsch, D. Kolarich, I. B. Wilson, F. Altmann, M. Duchene, *PLoS Biol.*, 2007, 5, e211.

[13] A. Muller-Schiffmann, J. Marz-Berberich, A, Andreyeva, R. Ronicke, D. Bartnik, O. Brener, J. Kutzsche, A. H. C. Horn, M. Hellmert, J. Polkowska, K. Gottmann, K. G. Reymann, S. A. Funke, L. Nagel-Steger, C. Moriscot, G. Schoehn, H. Sticht, D. Willbold, T. Schrader, C. Korth, *Angew. Chem. Int. Ed.*, 2010, 49, 8743.

[14] E. Lukevits, L. Demicheva, *Chemistry of Heterocyclic Compounds*, 1993, 29, 243.

[15] V. Tiwari, S. Verma, S. K. Verma, J. S. Dangi, *Eur. J. Pharm. Sci.*, 2016, 86, 50.

[16] (a) M. Abid, K. Husain, A. Azam, *Bioorg. Med. Chem. Lett*., 2005, 15, 4375. (b) S. Sharma, F. Athar, M. R. Maurya, F. Naqvi, A. Azam, *Eur. J. Med. Chem.*, 2005, 40, 557. (c) D. Bahl, F. Athar, M. B. P. Soares, M. Santos de Sá, D. R. M. Moreira, R. M. Srivastava, A. C. L. Leite, Amir Azam, *Bioorg. Med. Chem.*, 2010, 18, 6857.

[17] M. Mushtaque, F. Avecilla, A. Azam, *Eur. J. Med. Chem.*, 2012, 55, 439.

[18] A. K. Jain, A. Vaidya, V. Ravichandran, S. K. Kashaw, R. K. Agrawal, *Bioorg. Med. Chem.*, 2012, 20, 3378.

[19] Z. Guo, S-M Yiu and M. C. W. Chang, *Chem. A Eur. J.*, 2013, 19, 8937.

[20] M. R. Maurya, S. Dhaka and F. Avecila, *Polyhedron,* 2014, 81, 154.

[21] C. W. Wright, M. J. O'Neill, J. D. Phillipson, D. C. Warhurst, *Antimicrob. Agents Chemother.*, 1988, 32, 1725.

[22] T. Mosmann, *J. Immunol Methods*, 1983, 65, 55.

[23] T. F. Slater, *Biochim. Biophys. Acta*, 1963, 77, 365.

[24] V. Srimai, M. Ramesh, K. S. Parameshwar, T. Parthasarathy, *Med. Chem. Res.*, 2013, 22, 5314.

[25] C. A. Lipinski, *Drug Discovery Today: Technologies*, 2004, 4, 337.

[26] H. Van De Waterbeemd, E. Gifford, *Nature reviews Drug discovery*, 2003, 3, 192.

[27] C. de Graaf, N. P. E. Vermeulen, K. A. Feenstra, *J. Med. Chem.*, 2005, 48, 2725.

[28] P. Singh, F. Bast, *Med. Chem. Res*., 2014, 23, 1690.

[29] H. Pajouhesh, G. R. Lenz, *NeuroRx*, 2005, 2, 541.

[30] G. M. Morris, D. S. Goodsell, R. S. Halliday, R. Huey, W. E. Hart, R. K. Belew, A. J. Olson, *J. Comput. Chem.*, 1998, 19, 1639.

[31] C. Krishna, R. Jain, T. Kashav, D. Wadhwa, N. Alam, S. Gourinath, *Acta Crystallographica Section F Structural Biology and Crystallization Communications.*,

2007, 63, 512.

[32] G. M. Sheldrick, *SADABS*, version 2.10, University of Göttingen, Germany, 2004.

[33] G. M. Sheldrick, *SHELX*, *Acta Crystallogr. Sect. A*, 2008, 64, 112.

[34] L. S. Diamond, D. R. Harlow, C. C. Cunnick, *Trans. R. Soc. Trop. Med. Hyg.*, 1978, 72, 431.

[35] F. D. Gillin, D. S. Reiner, M. Suffness, *Antimicrob. Agents Chemother.*, 1982, 22, 342.

[36] J. Alexandre, P. Bleuzen, J. Bonneterre, W. Sutherland, J. L. Misset, J.-P. Guastalla, P. Viens, S. Faivre, A. Chahine, M. Spielman, A. Bensmaïne, M. Marty, M. Mahjoubi, E. Cvitkovic, *J. Clin. Oncol.*, 2000, 18, 562.

[37] H. E. Selick, A. P. Beresford, M. H. Tarbit, *Drug Discov. Today*, 2002, 2, 109.

[38] S. Kumar, I. Raj, I. Nagpal, N. Subbarao, S. Gourinath, *J. Biol. Chem.*, 2011, 286, 12533.

[39] I. Nagpal, I. Raj, N. Subbarao, S. Gourinath, *PLOS one*, 2012, 7, e30305.

Caption to Illustration

Caption Heading

Tables:

Table 1: Crystal Data and Structure Refinement for 3-(furan-2-ylmethyl)-2-(phenylimino)-1, 3-thiazolidin-4-one (**2**), for 5-(2, 5-dimethoxybenzylidene)-3-(furan-2-ylmethyl)-2-(phenylimino)-1, 3-thiazolidin-4-one (**6**), for 5-(4-hydroxybenzylidene)-3-(furan-2-ylmethyl)-2-(phenylimino)-1, 3-thiazolidin-4-one (**8**), for 5-(3-chlorobenzylidene)-3-(furan-2-ylmethyl)-2-(phenylimino)-1, 3-thiazolidin-4-one (**13**) and for 5-(4-isopropoxybenzylidene)-3-(furan-2-ylmethyl)-2-(phenylimino)-1, 3-thiazolidin-4-one (**15**)

Table 2: *In vitro* antiamoebic activity of Furan- Thiazolidinone hybrids (**1**-**17**) against HM1: IMSS strain of *E. histolytica*

Table 3: Binding energy and specific interaction of *Eh*TrR with compound

Table 4: Binding energy and specific interaction of *Eh*OASS with compounds

Figures:

Figure 1: Antiamoebic drug diloxanide furoate having furan ring

Figure 2: Furan based compounds having antiamoebic activity

Figure 3: Thiazolidinone derivatives with antiamoebic activity

Figure 4: General structure of Furan- thiazolidinone hybrids (blue and red colour depicts Furan and Thiazolidinone respectively)

Figure 5: ORTEP plot of compound 3-(furan-2-ylmethyl)-2-(phenylimino)-1, 3-thiazolidin-4-one (**2**). All the non-hydrogen atoms are presented by their 50% probability ellipsoids. Hydrogen atoms are omitted for clarity

Figure 6: ORTEP plot of compound 5-(2, 5-dimethoxybenzylidene)-3-(furan-2-ylmethyl)-2-(phenylimino)-1, 3-thiazolidin-4-one (**6**). All the non-hydrogen atoms are presented by their 50% probability ellipsoids. Hydrogen atoms are omitted for clarity

Figure 7: ORTEP plot of compound 5-(4-hydroxybenzylidene)-3-(furan-2-ylmethyl)-2-(phenylimino)-1, 3-thiazolidin-4-one (**8**). All the non-hydrogen atoms are presented by their 50% probability ellipsoids. Hydrogen atoms are omitted for clarity

Figure 8: ORTEP plot of compound 5-(3-chlorobenzylidene)-3-(furan-2-ylmethyl)-2-(phenylimino)-1, 3-thiazolidin-4-one (**13**). All the non-hydrogen atoms are presented by their 50% probability ellipsoids. Hydrogen atoms are omitted for clarity

Figure 9: ORTEP plot of compound 5-(4-isopropoxybenzylidene)-3-(furan-2-ylmethyl)-2-(phenylimino)-1, 3-thiazolidin-4-one (**15**). All the non-hydrogen atoms are presented by their 50% probability ellipsoids. Hydrogen atoms are omitted for clarity

Figure 10: π-π-stacking interactions between π clouds of thiazolidinone groups of different frameworks in compound 3-(furan-2-ylmethyl)-2-(phenylimino)-1, 3-thiazolidin-4-one (**2**)

Figure 11: π-π-stacking interactions between π clouds of thiazolidinone groups of different frameworks in compound 5-(4-hydroxybenzylidene)-3-(furan-2-ylmethyl)-2-(phenylimino)-1, 3-thiazolidin-4-one (**8**)

Figure 12: π-π-stacking interactions between π clouds around of dimethoxybenzylidene and thiazolidinone groups of different frameworks in compound 5-(2, 5-dimethoxybenzylidene)-3-(furan-2-ylmethyl)-2-(phenylimino)-1, 3-thiazolidin-4-one (**6**)

Figure 13: π-π-stacking interactions between π clouds of chlorobenzylidene and thiazolidinone groups of different frameworks in compound 5-(3-chlorobenzylidene)-3-(furan-2-ylmethyl)-2-(phenylimino)-1, 3-thiazolidin-4-one (**13**)

Figure 14: π-π-stacking interactions between π clouds of isopropoxybenzylidene and thiazolidinone groups of different frameworks in compound 5-(4-isopropoxybenzylidene)-3-(furan-2-ylmethyl)-2-(phenylimino)-1, 3-thiazolidin-4-one (**15**)

Figure 15: Assessment of viability of CHO normal cells in response to different compounds. Cells were plated in triplicates for 48 h and 72 h and treated with the compounds. Cells treated with DMSO are used as the control. MTT was added after completion of stipulated time intervals and processed. Absorbance was taken at 570 nm. Results were plotted taking control (DMSO) as 100%

Figure 16: (A & B) Protein ligands interaction profile of *Eh*TrR with reference compounds (Metronidazole [MNZ] and 2-{1-[2-(2-Methyl-5-nitro-imidazol-1-yl)-ethyl]-*1H*-[1,2,3]triazol-4-yl}-pyridine [A]). C. Protein ligands interaction profile of *Eh*TrR with compound **3**. D. Protein ligands interaction profile of *Eh*TrR with compound **6**. E. Protein ligands interaction profile of *Eh*TrR with compound **8**. F. Protein ligands interaction profile of *Eh*TrR with compound **11**. G. Protein ligands interaction profile of *Eh*TrR with compound **12**. H. Protein ligands interaction profile of *Eh*TrR with compound **14**. I. Protein ligands interaction profile of *Eh*TrR with compound **16**

Figure 17: (A & B) Protein ligands interaction profile of *Eh*OASS with reference compounds (Metronidazole [MNZ] and 4-hydroxy-2-[2-(1H-indol-3-yl)-2-oxoethyl]sulfanyl- 1H-pyrimidin-6-one [W]). C. Protein ligands interaction profile of *Eh*OASS with compound **3**. D. Protein ligands interaction profile of *Eh*OASS with compound **6**. E. Protein ligands interaction profile of *Eh*OASS with compound **8**. F. Protein ligands interaction profile of

*Eh*OASS with compound **11**. G. Protein ligands interaction profile of *Eh*OASS with compound **12**. H. Protein ligands interaction profile of *Eh*OASS with compound **14**. I. Protein ligands interaction profile of *Eh*OASS with compound **16**

Figure 18: Plot for % inhibition versus log of inhibition concentration for enzyme O-acetyle-L-serine sulfohydrolase

Scheme:

Scheme 1: Synthesis of Furan- thiazolidinone hybrids (**3**-**17**)

Table 1: Crystal Data and Structure Refinement for 3-(furan-2-ylmethyl)-2-(phenylimino)-1, 3-thiazolidin-4-one (**2**), for 5-(2, 5-dimethoxybenzylidene)-3-(furan-2-ylmethyl)-2-(phenylimino)-1, 3-thiazolidin-4-one (**6**), for 5-(4-hydroxybenzylidene)-3-(furan-2-ylmethyl)-2-(phenylimino)-1, 3-thiazolidin-4-one (**8**), for 5-(3-chlorobenzylidene)-3-(furan-2-ylmethyl)-2-(phenylimino)-1, 3-thiazolidin-4-one (**13**) and for 5-(4-isopropoxybenzylidene)-3-(furan-2-ylmethyl)-2-(phenylimino)-1, 3-thiazolidin-4-one (**15**)

	2	**6**	**8**	**13**	**15**
Formula	$C_{14}H_{12}N_2O_2S$	$C_{23}H_{20}N_2O_4S$	$C_{24}H_{22}N_2O_3S$	$C_{21}H_{15}ClN_2O_2S$	$C_{24}H_{22}N_2O_3S$
Formula weight	272.32	420.47	418.50	394.86	418.50
T, *K*	100(2)	100(2)	100(2)	100(2)	100(2)
Wavelength, Å	0.71073	0.71073	0.71073	0.71073	0.71073
Crystal system	Monoclinic	Monoclinic	Monoclinic	Monoclinic	Triclinic
Space group	$P2_1/c$	$P2_1/n$	$P2_1/c$	$P2_1/c$	$P\bar{1}$
a/Å	9.4895(12)	11.1942(5)	9.3960(3)	13.6225(11)	9.4666(4)
b/Å	10.0835(13)	15.5030(6)	38.5335(13)	9.8426(8)	9.6143(5)
c/Å	13.3165(17)	12.8047(5)	11.7872(4)	14.3378(11)	12.8356(9)
α/°					105.172(4)
β/°	93.067(6)	115.112(2)	95.081(2)	111.344(3)	106.844(4)
γ/°					101.394(3)
V/Å^3	1272.4(3)	2012.13(14)	4250.9(2)	1790.6(2)	1030.79(10)
Z	4	4	8	4	2
F_{000}	*568*	880	1760	816	440

D_{calc}/g cm^{-3}	1.422	1.388	1.308	1.465	1.348
μ/mm^{-1}	0.253	0.194	0.180	0.350	0.186
θ/ (º)	2.53 to 30.68	2.03 to 28.39	1.81 to 24.41	2.57 to 30.63	1.76 to 27.10
R_{int}	0.0409	0.0382	0.0838	0.0355	0.0486
Crystal size/ mm^3	0.49 x 0.26 x 0.21	0.48 x 0.33 x 0.19	0.40 x 0.35 x 0.22	0.48 x 0.46 x 0.45	0.37 x 0.26 x 0.13
Goodness-of-fit on F^2	1.046	1.048	1.050	1.113	1.097
$R_1[I>2\sigma(I)]$ [a]	0.0319	0.0342	0.0436	0.0344	0.0396
wR_2 (all data) [b]	0.0883	0.0895	0.1199	0.0948	0.1210
Largest differences peak and hole (eÅ^{-3})	0.415 and -0.215	0.343 and -0.287	0.657 and -0.584	0.689 and -0.577	0.533 and -0.344

[a] $R_1 = \Sigma \left| |F_o| - |F_c| \right| / \Sigma |F_o|$. [b] $wR_2 = \{\Sigma[w(|F_o|^2 - |F_c|^2)^2] / \Sigma[w(F_o^2)^2]\}^{1/2}$

Table 2: *In vitro* antiamoebic activity of Furan-thiazolidinone hybrids against HM1: IMSS strain of *E. histolytica*

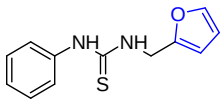

(1)

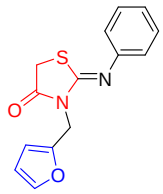

(2)

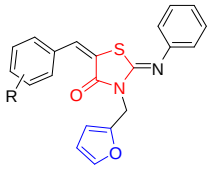

(3-17)

Compound No.	**Ar-R**	**Antiamoebic Activity IC_{50}(µM)±S.D.**	**Cytotoxicity (48 hrs) IC_{50}(µM)±S.D.**	**Cytotoxicity (72 hrs) IC_{50}(µM)±S.D.**	**Inhibition assay IC_{50} (µM)**
1	-	8.22±0.007	N.D	N.D	N.D
2	-	3.57±0.006	N.D	N.D	N.D
3	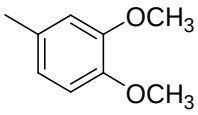	**0.47**±0.004	>400	>250	157.5
4	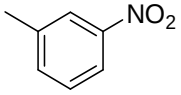	1.95±0.003	N.D	N.D	N.D
5	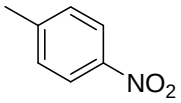	2.87±0.003	N.D	N.D	N.D
6	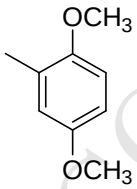	**0.67**±0.042	>400	>250	144.3
7	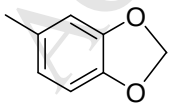	2.97±0.031	N.D	N.D	N.D
8	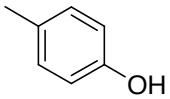	**1.04**±0.023	400 ±0.29	>250	N.D
9	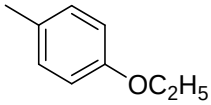	2.03±0.023	N.D	N.D	N.D

10	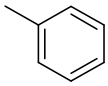	2.25±0.058	N.D	N.D	N.D
11	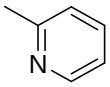	**0.27**±0.047	>400	>250	137.9
12	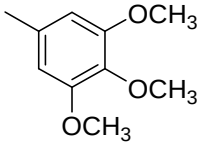	**1.24**±0.038	>400	>250	N.D
13	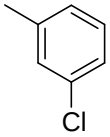	1.95±0.035	N.D	N.D	N.D
14	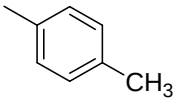	**1.48**±0.007	421± 0.14	185±0.22	N.D
15	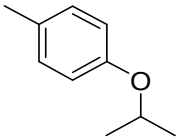	2.20±0.004	N.D	N.D	N.D
16	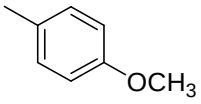	**1.35**±0.003	>400	>250	N.D
17	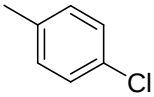	2.33±0.002	N.D	N.D	N.D
18	Metronidazole	1.64±0.006	>400	280±0.19	N.D

[a] The values obtained in at least three separate assays done in triplicate
[b] Standard Deviation

Table 3: Binding energy and specific interaction of *Eh*TrR with compound

Compound no.	Binding energy(kcal/mol)	Inhibitory constant(μM)	Protein ligands interaction		
			No. of H bonds	Amino acid residues	Distance (Å)
2	-4.74	337.07	1	GLN-292	3.1
3	-8.41	0.68	1	VAL-289	3.3
4	-7.43	3.56	3	HIS-248	3.0, 3.2 and 3.5
5	-6.54	16.14	-	-	-
6	-8.40	0.69	4	THR-269 and ARG-269	3.6, 3.1,3.0 and 3.1
7	-6.23	27.00	2	TYR-266 and HIS-248	3.0 and 3.2
8	-8.37	0.73	2	HIS-248 and ARG-291	2.3 and 3.3
9	-7.27	4.66	2	LYS-309 and TYR-290	3.4 and 3.1
10	-6.77	10.89	-	-	-
11	-8.73	0.39	-	-	-
12	-8.16	1.05	1	ARG-188	2.8
13	-7.42	3.16	3	GLN-292, ASN-55 and ARG-25	3.0, 3.1 and 3.3
14	-7.57	2.82	3	ARG-291,GLN-292 and TYR-292	3.3, 3.3 and 3.2
15	-7.16	5.68	2	ARG-25	3.0 and 3.3
16	-7.76	2.07	1	ARG-25	3.1
17	-7.10	6.23	1	ARG-188	3.4
MNZ	-7.48	3.30	5	HIS-248,ARG-291 and ASP-284	3.2, 3.5, 3.3, 2.7 and3.4
A	-7.56	2.88	5	GLN-292, ASN-55 and ARG-25	3.2, 3.0, 3.1, 3.0 and 3.1

Table 4: Binding energy and specific interaction of *Eh*OASS with compounds

Compound no.	Binding energy (kcal/mol)	Inhibitory constant (µM)	Protein ligands interaction		
			No. of H bonds	Amino acid residues	Distance (Å)
2	3.61	2240	1	LYS-327	3.1
3	-6.69	12.37	1	ASN-16	3.2
4	5.91	46.76	1	THR-89	3.2
5	5.47	98.61	-	-	-
6	-6.67	12.84	1	TYR-319	3.5
7	4.73	342.78	1	LEU-127	3.2
8	-6.56	15.66	-	-	-
9	5.18	148.89	1	HIS-30	3.1
10	-5.78	58.03	1	HIS-30	2.8
11	-6.74	11.54	3	THR-33,HIS-30 and LEU-29	3.4, 3.0 and 3.5
12	-6.38	21.95	2	SER-86	3.4 and 3.2
13	5.91	45.76	1	LYS-271	3.1
14	-6.69	12.37	-	-	-
15	-5.72	54.78	1	HIS-30	2.9
16	-6.39	20.90	1	THR-33	3.1
17	5.56	84.29	1	SER-84	3.1
MNZ	-5.96	42.61	4	ARG-116, GLU-115 and SER-315	3.1, 2.8, 3.1 and 2.7
W	-6.26	25.58	6	GLU-311, GLU-311, GLU-115, LEU-314 and SER-315	3.4, 3.4,2.6, 3.2, 3.3 and 3.5

Figure 1: Antiamoebic drug Diloxanide furoate having Furan ring

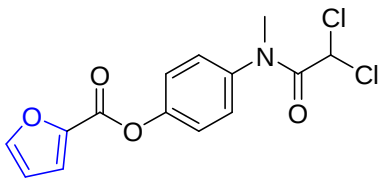

Figure 2: Furan based compounds having antiamoebic activity

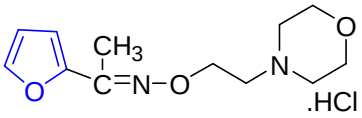

IC_{50} = 0.60µM

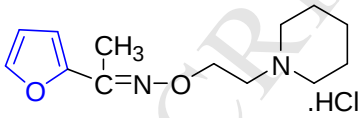

IC_{50} = 1.70µM

Figure 3: Thiazolidinone derivatives with antiamoebic activity

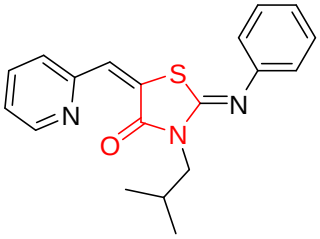

IC_{50} = 0.60µM

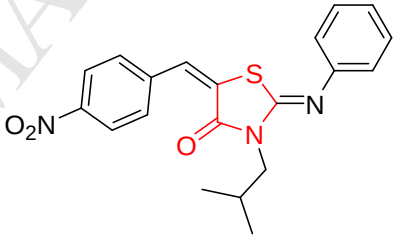

IC_{50} = 0.13µM

Figure 4: General structure of Furan-thiazolidinone hybrids (blue and red color depicts Furan and Thiazolidinone respectively)

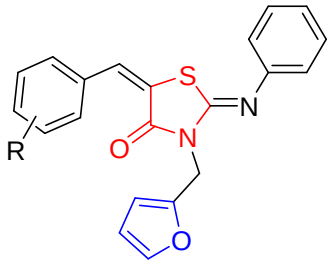

Figure 5: ORTEP plot of compound **3-(furan-2-ylmethyl)-2-(phenylimino)-1, 3-thiazolidin-4-one (2)**. All the non-hydrogen atoms are presented by their 50% probability ellipsoids. Hydrogen atoms are omitted for clarity

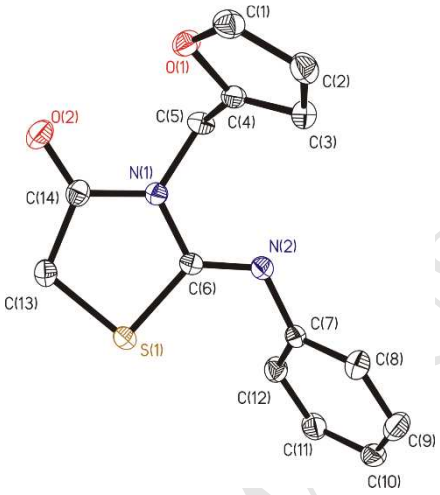

Figure 6: ORTEP plot of compound **5-(2, 5-dimethoxybenzylidene)-3-(furan-2-ylmethyl)-2-(phenylimino)-1, 3-thiazolidin-4-one (6)**. All the non-hydrogen atoms are presented by their 50% probability ellipsoids. Hydrogen atoms are omitted for clarity

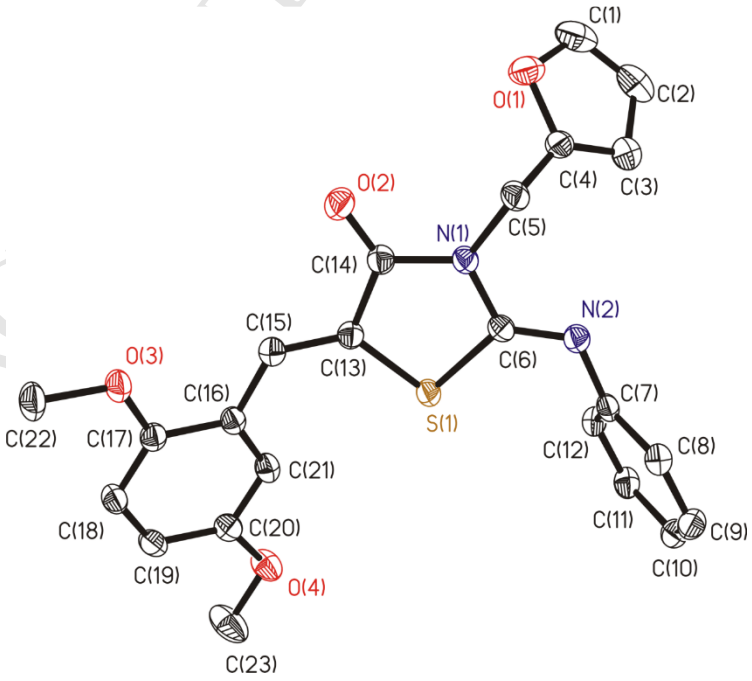

Figure 7: ORTEP plot of compound **5-(4-hydroxybenzylidene)-3-(furan-2-ylmethyl)-2-(phenylimino)-1, 3-thiazolidin-4-one (8)**. All the non-hydrogen atoms are presented by their 50% probability ellipsoids. Hydrogen atoms are omitted for clarity

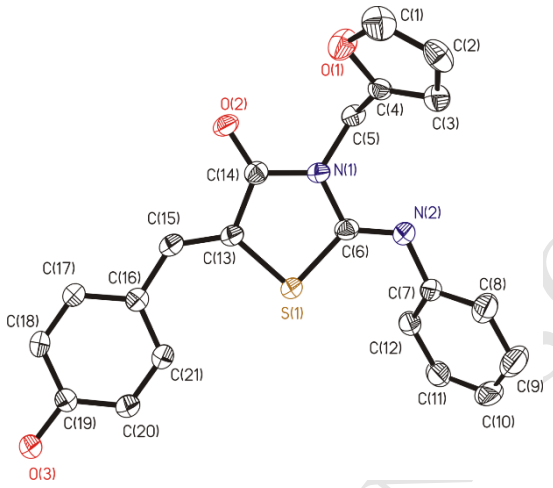

Figure 8: ORTEP plot of compound **5-(3-chlorobenzylidene)-3-(furan-2-ylmethyl)-2-(phenylimino)-1, 3-thiazolidin-4-one (13)**. All the non-hydrogen atoms are presented by their 50% probability ellipsoids. Hydrogen atoms are omitted for clarity

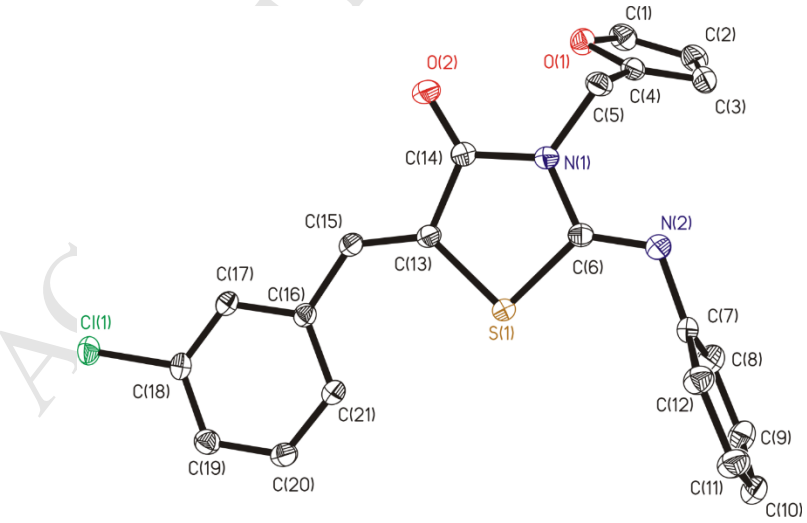

Figure 9: ORTEP plot of compound **5-(4-isopropoxybenzylidene)-3-(furan-2-ylmethyl)-2-(phenylimino)-1, 3-thiazolidin-4-one (15)**. All the non-hydrogen atoms are presented by their 50% probability ellipsoids. Hydrogen atoms are omitted for clarity

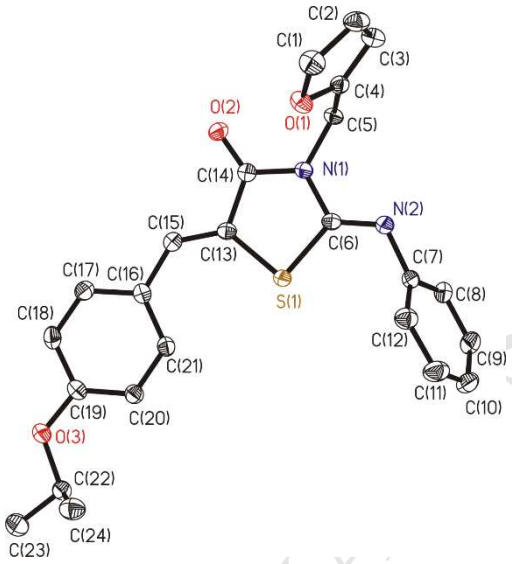

Figure 10: π-π-stacking interactions between π clouds of thiazolidinone groups of different frameworks in compound **3-(furan-2-ylmethyl)-2-(phenylimino)-1, 3-thiazolidin-4-one** (**2**)

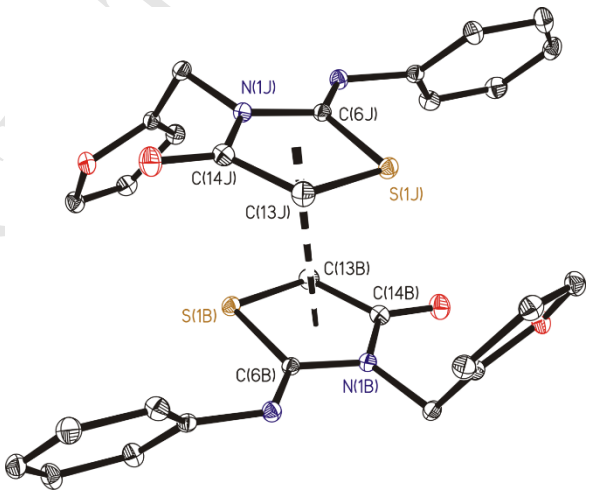

Figure 11: π-π-stacking interactions between π clouds of thiazolidinone groups of different frameworks in compound **5-(4-hydroxybenzylidene)-3-(furan-2-ylmethyl)-2-(phenylimino)-1, 3-thiazolidin-4-one** (**8**)

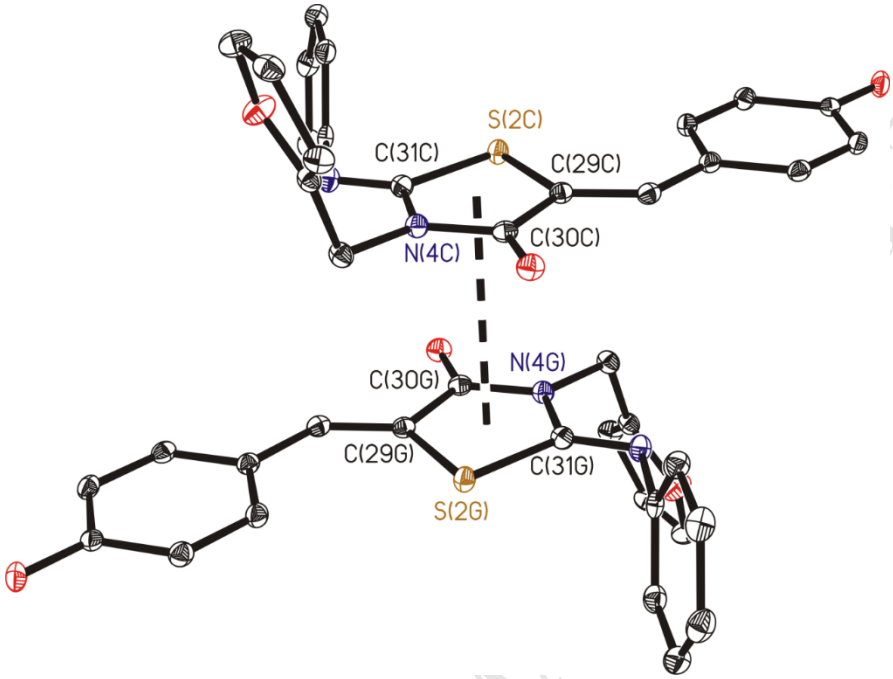

Figure 12: π-π-stacking interactions between π clouds around of dimethoxybenzylidene and thiazolidinone groups of different frameworks in compound **5-(2, 5-dimethoxybenzylidene)-3-(furan-2-ylmethyl)-2-(phenylimino)-1, 3-thiazolidin-4-one** (**6**)

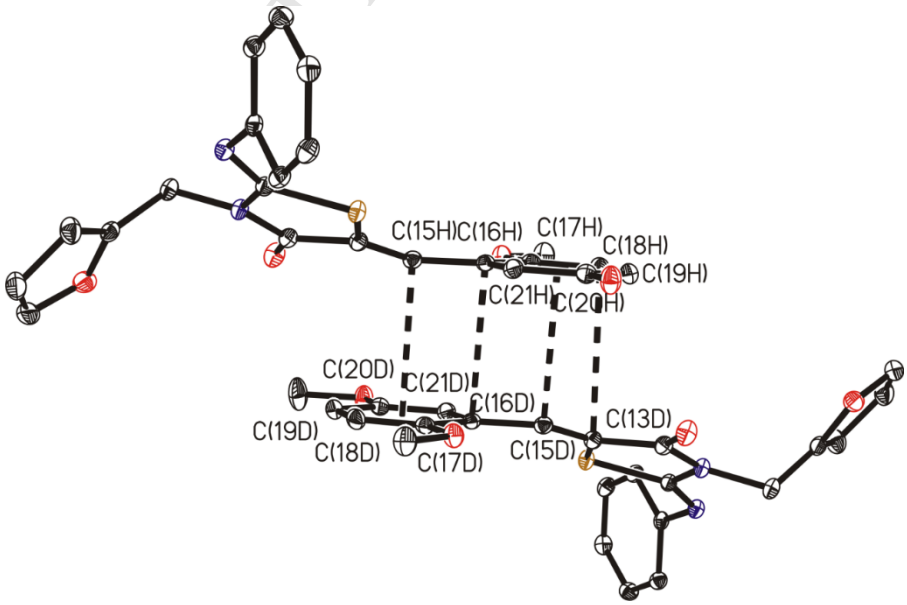

Figure 13: π-π-stacking interactions between π clouds of chlorobenzylidene and thiazolidinone groups of different frameworks in compound **5-(3-chlorobenzylidene)-3-(furan-2-ylmethyl)-2-(phenylimino)-1, 3-thiazolidin-4-one** (**13**)

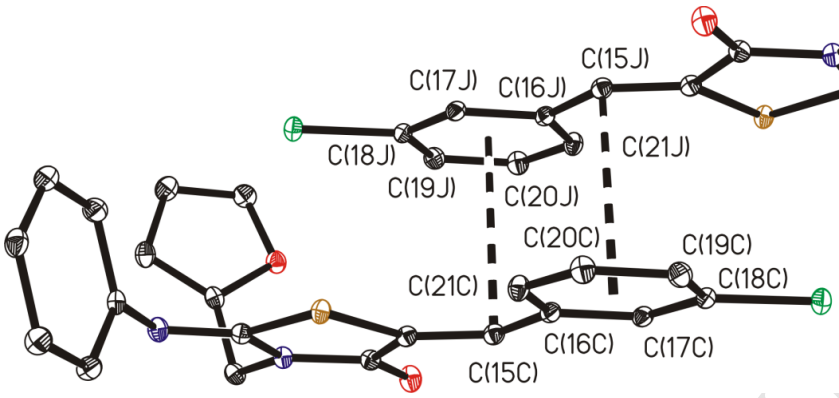

Figure 14: π-π-stacking interactions between π clouds of isopropoxybenzylidene and thiazolidinone groups of different frameworks in compound **5-(4-isopropoxybenzylidene)-3-(furan-2-ylmethyl)-2-(phenylimino)-1, 3-thiazolidin-4-one** (**15**)

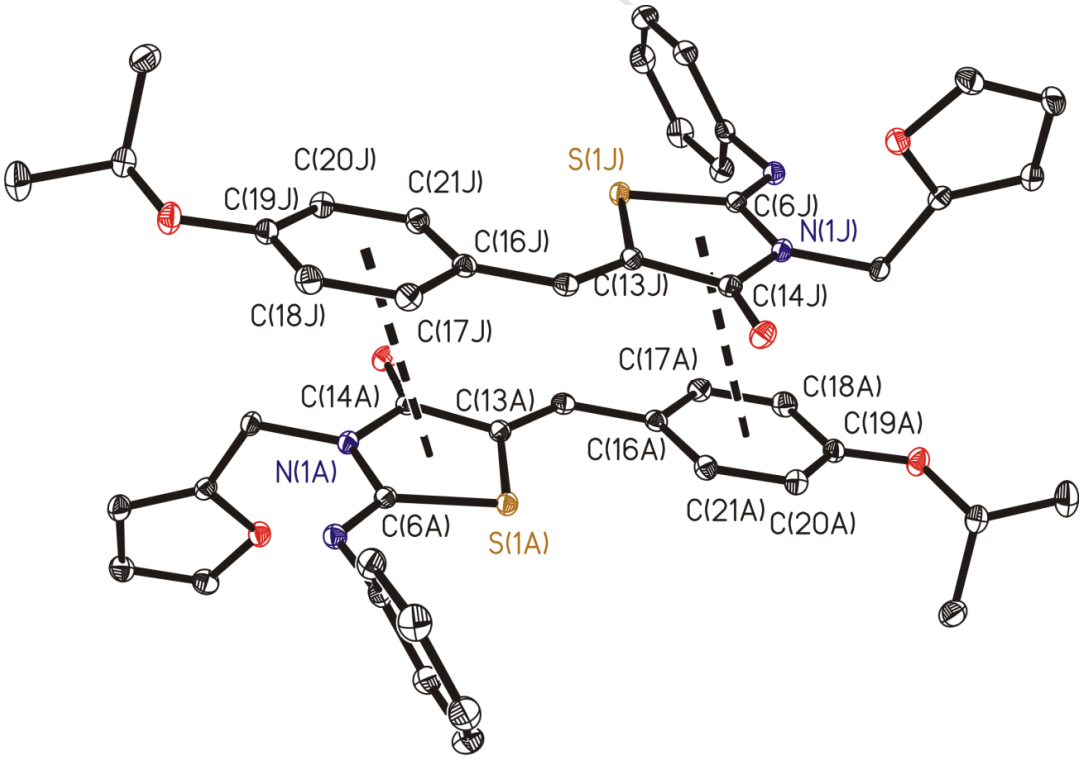

Figure 15: Assessment of viability of CHO normal cells in response to different compounds. Cells were plated in triplicates for 48 h and 72 h and treated with the compounds. Cells treated with DMSO was used as the control. MTT was added after completion of stipulated time intervals and processed. Absorbance was taken at 570 nm. Results were plotted taking control (DMSO) as 100%

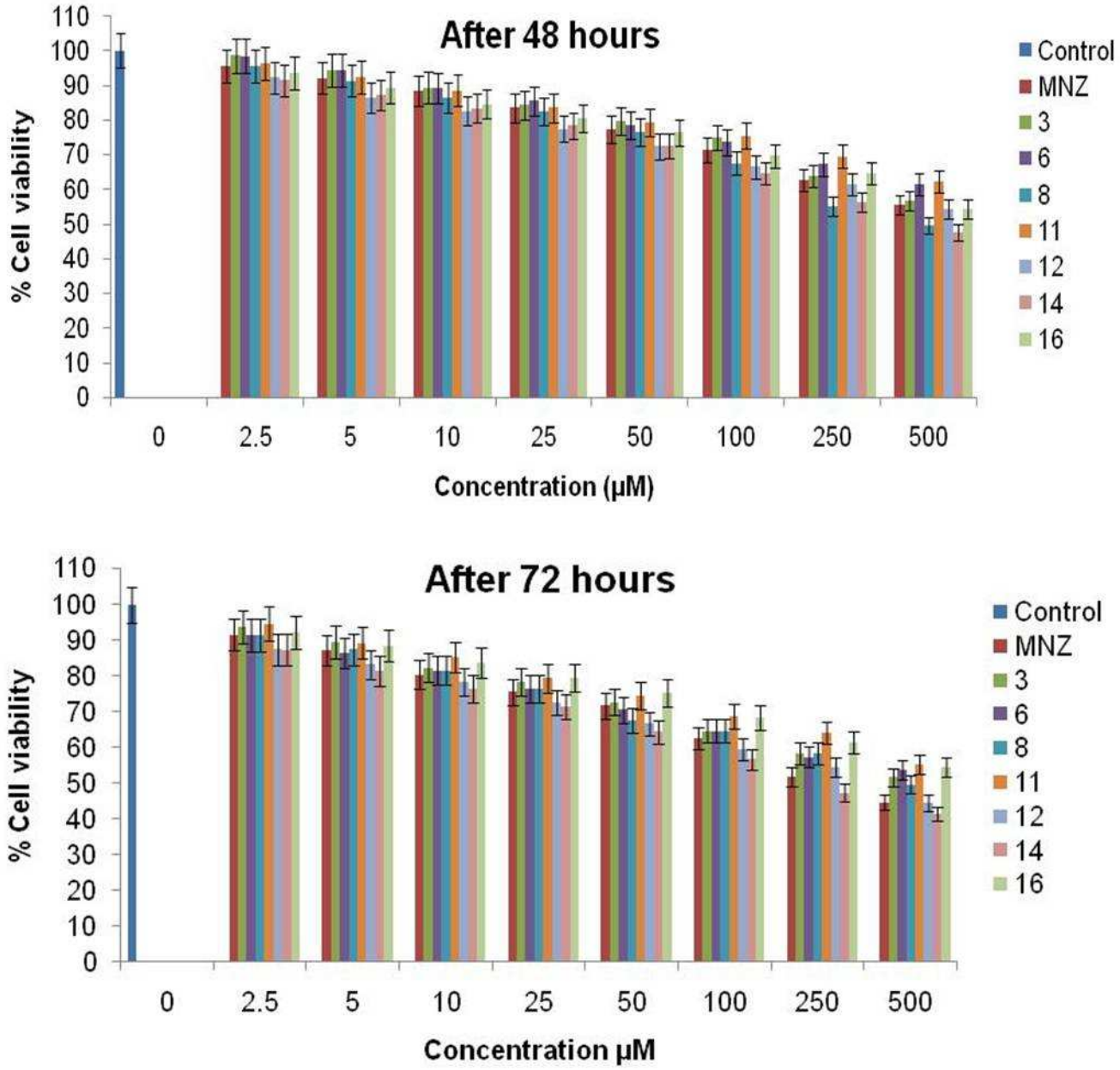

Figure 16: (**A & B)** Protein ligands interaction profile of *Eh*TrR with reference compounds (Metronidazole [MNZ] and 2-{1-[2-(2-Methyl-5-nitro-imidazol-1-yl)-ethyl]-*1H*-[1,2,3]triazol-4-yl}-pyridine [A]). **C.** Protein ligands interaction profile of *Eh*TrR with compound **3**. **D**. Protein ligands interaction profile of *Eh*TrR with compound **6. E.** Protein ligands interaction profile of *Eh*TrR with compound **8**. **F.** Protein ligands interaction profile of *Eh*TrR with compound **11**. **G.** Protein ligands interaction profile of *Eh*TrR with compound **12. H.** Protein ligands interaction profile of *Eh*TrR with compound **14**. **I.** Protein ligands interaction profile of *Eh*TrR with compound **16**

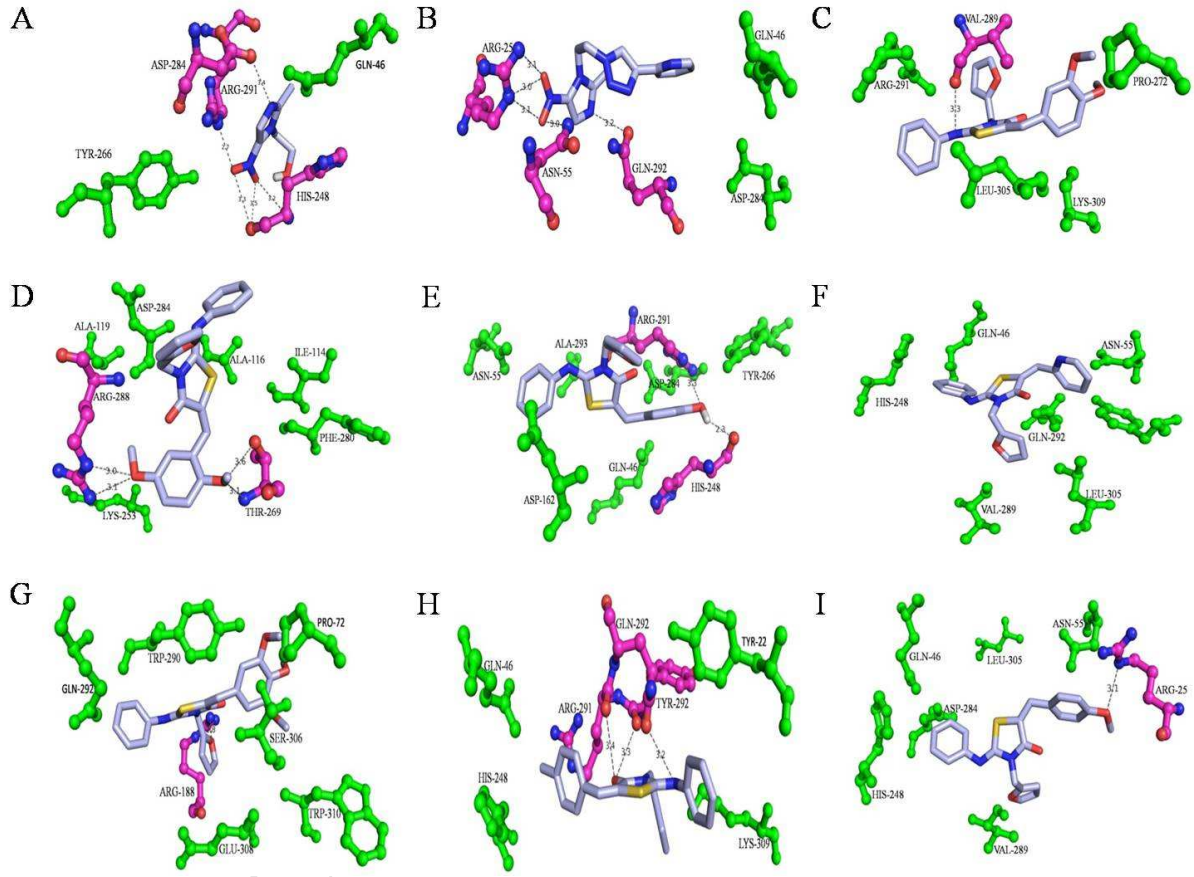

Figure 17: (**A & B)** Protein ligands interaction profile of *Eh*OASS with reference compounds (Metronidazole [MNZ] and 4-hydroxy-2-[2-(1H-indol-3-yl)-2-oxoethyl]sulfanyl- 1H-pyrimidin-6-one [W]). **C.** Protein ligands interaction profile of *Eh*OASS with compound **3**. **D**. Protein ligands interaction profile of *Eh*OASS with compound **6. E.** Protein ligands interaction profile of *Eh*OASS with compound **8**. **F.** Protein ligands interaction profile of *Eh*OASS with compound **11**. **G.** Protein ligands interaction profile of *Eh*OASS with compound **12. H.** Protein ligands interaction profile of *Eh*OASS with compound **14**. **I.** Protein ligands interaction profile of *Eh*OASS with compound **16**

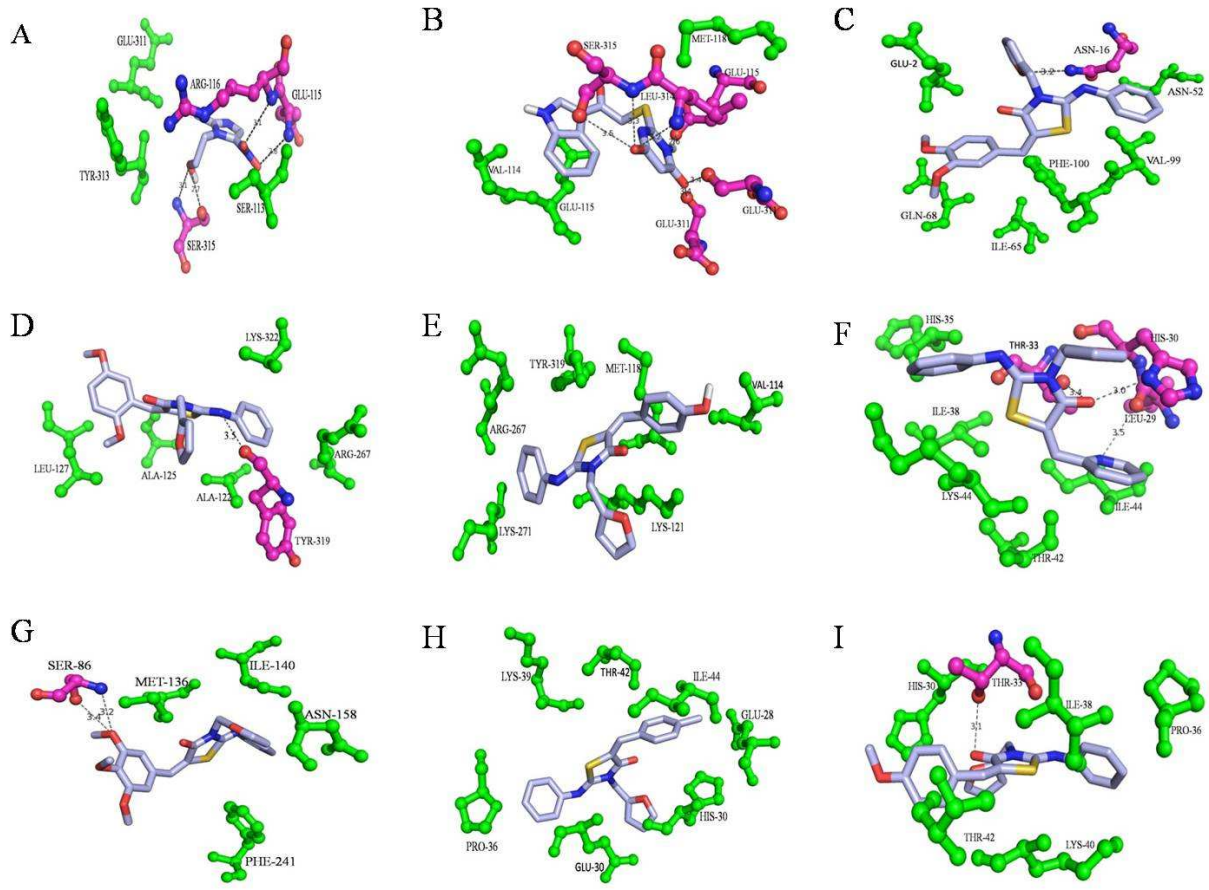

Figure 18: Plot for % inhibition versus log of inhibition concentration for enzyme O-acetyle-L-serine sulfohydrolase

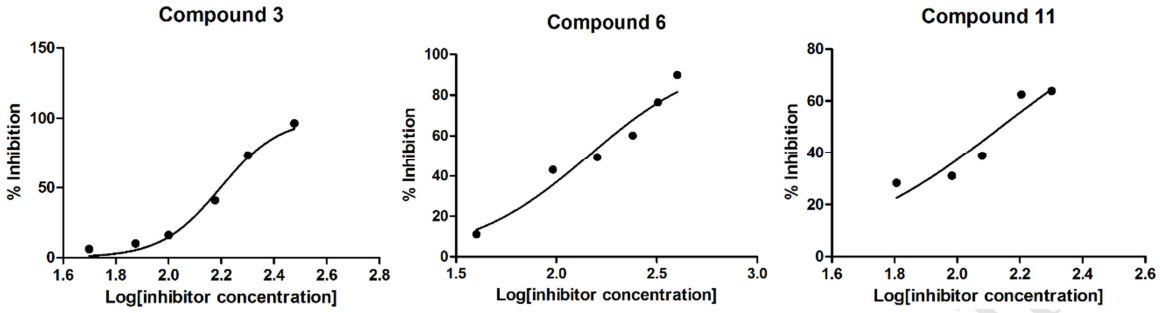

Scheme 1: Synthesis of Furan- Thiazolidinone hybrids (**3-17**)

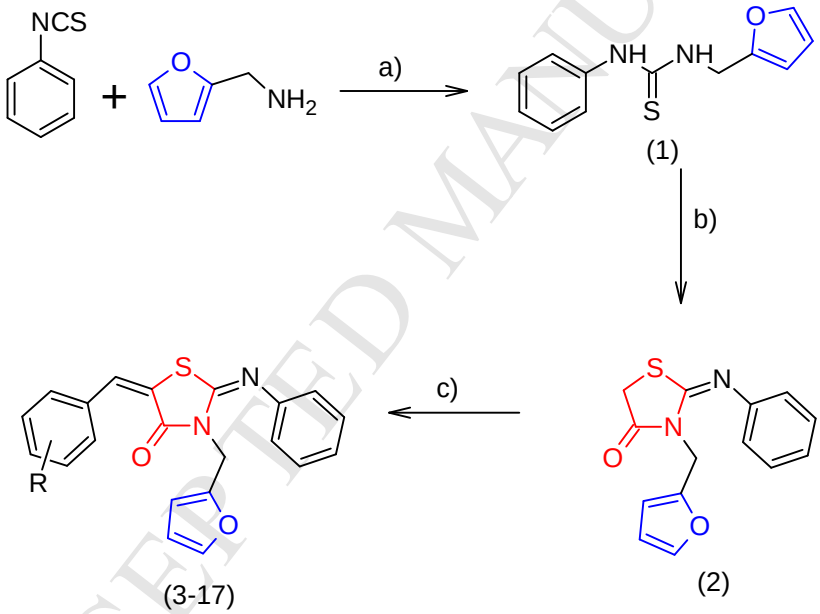

Reagents and conditions: *a) Toluene, room temperature, 1h. b) Anhydrous sodium acetate, chloroacetic acid, ethanol, reflux, 14 h. c) Piperidine, ethanol, reflux, 12-16 h.*

Research Highlights

- Furan-thiazolidinone hybrids were synthesized.
- Compounds were evaluated for antiamoebic activity.
- Compounds showed growth inhibitory effect on Chinese hamster ovary cells.
- Molecular docking study was performed on *Eh*TrR *and Eh*OASS.
- Three compounds showed most promising antiamoebic activity and significant inhibition on O-acetyle-L-serine sulfohydrolase